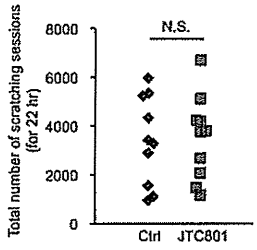

FIG E7. Scratching behavior in NC/Nga mice. The number of scratching sessions for 22 hours after JTC801 (30 mg/kg in 0.5% methyl cellulose) or vehicle treatment (n = 10) is shown. These results are a representative of 2 independent experiments. *N.S.*, Not significant.

TABLE E1. Some compounds included in the Tocriscreen Mini promote *FLG* expression levels

Compound	Mechanism of action	Relative
Scriptaid	Histone deacetylase inhibitor	381.8
JTC801	ORL1 antagonist	22.7
Actinomycin D	Antineoplastic antibiotic	20.5
MG132	Proteasome and calpain inhibitor; inhibits nuclear factor κB activation	18.4
LE135	Retinoic acid receptor-β antagonist	17.1
A23187, free acid	Calcium ionophore	15.7
Ryuvidine	Cyclin-dependent kinase 4 (cdk4) inhibitor	10.5

The compounds included in the Tocriscreen Mini were screened for *FLG* production by HaCaT cells by means of real-time PCR. The relative value was calculated as the relative expression of *FLG* treated with each compound divided by the relative expression of *FLG* without compound treatment.

TABLE E2. Clinical observation

	Control	JTC801
Right ear	3.9 ± 1.7	1.4 ± 1.0
Left ear	3.8 ± 1.5	1.6 ± 1.3
Dorsum	3.3 ± 1.3	1.5 ± 1.4
Face	2.6 ± 1.6	1.5 ± 1.3

The clinical severity of skin lesions was scored according to the macroscopic diagnostic criteria that were used for NC/Nga mice. The scores in the right ear, left ear, dorsum, and face were the sum of individual scores, which were graded as 0 (none), 1 (mild), and 2 (severe) for the symptoms of erythema/hemorrhage, edema, crust, excoriation/erosion, and scaling/dryness.

nature immunology

Perivascular leukocyte clusters are essential for efficient activation of effector T cells in the skin

Yohei Natsuaki[1,2,15], Gyohei Egawa[1,15], Satoshi Nakamizo[1], Sachiko Ono[1], Sho Hanakawa[1], Takaharu Okada[3], Nobuhiro Kusuba[1], Atsushi Otsuka[1], Akihiko Kitoh[1], Tetsuya Honda[1], Saeko Nakajima[1], Soken Tsuchiya[4], Yukihiko Sugimoto[4], Ken J Ishii[5,6], Hiroko Tsutsui[7], Hideo Yagita[8], Yoichiro Iwakura[9,10], Masato Kubo[11,12], Lai guan Ng[13], Takashi Hashimoto[2], Judilyn Fuentes[14], Emma Guttman-Yassky[14], Yoshiki Miyachi[1] & Kenji Kabashima[1]

It remains largely unclear how antigen-presenting cells (APCs) encounter effector or memory T cells efficiently in the periphery. Here we used a mouse contact hypersensitivity (CHS) model to show that upon epicutaneous antigen challenge, dendritic cells (DCs) formed clusters with effector T cells in dermal perivascular areas to promote *in situ* proliferation and activation of skin T cells in a manner dependent on antigen and the integrin LFA-1. We found that DCs accumulated in perivascular areas and that DC clustering was abrogated by depletion of macrophages. Treatment with interleukin 1α (IL-1α) induced production of the chemokine CXCL2 by dermal macrophages, and DC clustering was suppressed by blockade of either the receptor for IL-1 (IL-1R) or the receptor for CXCL2 (CXCR2). Our findings suggest that the dermal leukocyte cluster is an essential structure for elicitating acquired cutaneous immunity.

Boundary tissues, including the skin, are continually exposed to foreign antigens, which must be monitored and possibly eliminated. Upon exposure to foreign antigens, skin dendritic cells (DCs), including epidermal Langerhans cells (LCs), capture the antigens and migrate to draining lymph nodes (LNs), where the presentation of antigen to naive T cells occurs mainly in the T cell zone. In this location, the accumulation of naive T cells in the vicinity of DCs is mediated by signaling via the chemokine receptor CCR7 (ref. 1). The T cell zone in the draining LNs facilitates the efficient encounter of antigen-bearing DCs with antigen-specific naive T cells.

In contrast to T cells in LNs, the majority of T cells in the skin, including infiltrating skin T cells and skin-resident T cells, have an effector-memory phenotype[2]. In addition, the presentation of antigen to skin T cells by antigen-presenting cells (APCs) is the crucial step in the elicitation of acquired skin immune responses, such as contact dermatitis. Therefore, we investigated how antigen presentation occurs in the skin and if it is different from antigen presentation in LNs. Published studies using mouse contact hypersensitivity (CHS) as a model of human contact dermatitis have revealed that dermal DCs (dDCs) have a pivotal role in the transport and presentation of antigen to the LNs, but epidermal LCs do not[3]. In the skin, however, it remains unclear which subset of APCs presents antigens to skin T cells and how skin T cells efficiently encounter APCs. In addition, dermal macrophages are key modulators in CHS responses[4], but the precise mechanisms by which macrophages are involved in the recognition of antigen in the skin have not yet been clarified. These unanswered questions prompted us to investigate where skin T cells recognize antigens and how skin T cells are activated in the elicitation phase of acquired cutaneous immune responses such as CHS.

When keratinocytes encounter foreign antigens, they immediately produce various proinflammatory mediators, such as interleukin 1 (IL-1) and tumor-necrosis factor, in an antigen-nonspecific manner[5,6]. Proteins of the IL-1 family are considered important modulators in CHS responses because the activation of hapten-specific T cells is impaired in mice deficient in both IL-1α and IL-1β but not in mice deficient in tumor-necrosis factor[7]. IL-1α and IL-1β are agonistic ligands of the receptor for IL-1 (IL-1R). While IL-1α is stored in keratinocytes and is secreted upon exposure to nonspecific stimuli, IL-1β is produced mainly by epidermal LCs and dermal mast cells in an inflammasome-dependent manner via activation of the cytoplasmic pattern-recognition receptor NLRP3 and of caspase-1 and caspase-11. Because IL-1α and IL-1β are crucial in the initiation of acquired

[1]Department of Dermatology, Kyoto University Graduate School of Medicine, Kyoto, Japan. [2]Department of Dermatology, Kurume University School of Medicine, Fukuoka, Japan. [3]Research Unit for Immunodynamics, RIKEN Research Center for Allergy and Immunology, Kanagawa, Japan. [4]Department of Pharmaceutical Biochemistry, Graduate School of Pharmaceutical Sciences, Kumamoto University, Kumamoto, Japan. [5]Laboratory of Adjuvant Innovation, National Institute of Biomedical Innovation, Osaka, Japan. [6]Laboratory of Vaccine Science, WPI Immunology Frontier Research Center, Osaka University, Osaka, Japan. [7]Department of Microbiology, Hyogo College of Medicine, Hyogo, Japan. [8]Department of Immunology, Juntendo University School of Medicine, Tokyo, Japan. [9]Research Institute for Biomedical Sciences, Tokyo University of Science, Chiba, Japan. [10]Medical Mycology Research Center, Chiba University, Chiba, Japan. [11]Laboratory for Cytokine Regulation, RIKEN center for Integrative Medical Science, Kanagawa, Japan. [12]Division of Molecular Pathology, Research Institute for Biomedical Science, Tokyo University of Science, Chiba, Japan. [13]Singapore Immunology Network, Agency for Science, Technology and Research, Biopolis, Singapore. [14]Department of Dermatology, Icahn School of Medicine at Mount Sinai School Medical Center, New York, New York, USA. [15]These authors contributed equally to this work. *Correspondence should be addressed to K.K. (kaba@kuhp.kyoto-u.ac.jp).*

Received 7 July; accepted 19 August; published online 21 September 2014; doi:10.1038/ni.2992

immune responses such as CHS, it is of great interest to understand how IL-1 modulates the recognition of antigen by skin T cells.

Using a mouse CHS model, here we examined how DCs and effector T cells encounter each other efficiently in the skin. We found that upon encountering antigenic stimuli, dDCs formed clusters in which effector T cells were activated and proliferated in an antigen-dependent manner. These DC–T cell clusters were initiated by skin macrophages via IL-1R signaling and were essential for the establishment of cutaneous acquired immune responses.

RESULTS

Formation of DC–T cell clusters at antigen-challenged sites

To explore the accumulation of cells of the immune system in the skin, we examined the clinical and histological features of the elicitation of human allergic contact dermatitis. Allergic contact dermatitis is the most common of eczematous skin diseases, affecting 15–20% of the general population worldwide[8], and is mediated by T cells. Although antigens should be spread evenly over the surface of skin, clinical manifestations commonly include discretely distributed small vesicles (**Fig. 1a**), which suggests an uneven occurrence of intense inflammation. Histological examination of allergic contact dermatitis showed spongiosis, intercellular edema in the epidermis and colocalization of perivascular infiltrates of $CD3^+$ T cells and spotty accumulation of $CD11c^+$ DCs in the dermis, especially beneath the vesicles (**Fig. 1b**). These findings led us to hypothesize that focal accumulation of T cells and DCs in the dermis might contribute to vesicle formation in early eczema.

To characterize the DC–T cell clusters in elicitation reactions, we used two-photon microscopy to obtain time-lapse images in a mouse model of CHS. We isolated T cells from the draining LNs of mice sensitized with the hapten DNFB (2,4-dinitrofluorobenzene), labeled the cells with fluorescent dye and transferred them into mice that express the common DC marker CD11c tagged with yellow fluorescent protein (YFP). In the steady state, YFP^+ dDCs distributed diffusely (**Fig. 1c**), representative of nondirected movement in a random fashion (**Supplementary Fig. 1**), as reported before[9]. After topical challenge with DNFB, YFP^+ dDCs transiently increased their velocity and formed clusters in the dermis, with the clusters becoming larger and more evident after 24 h (**Fig. 1c** and **Supplementary Movie 1**). At the same time, transferred T cells accumulated in the DC clusters and interacted with YFP^+ DCs for several hours (**Fig. 1d** and **Supplementary Movie 2**). Thus, we observed accumulation of DCs and T cells in the dermis in mice during CHS responses. We noted that the intercellular spaces between keratinocytes overlying the DC–T cell clusters in the dermis were enlarged (**Fig. 1e**), which replicated observations made for human allergic contact dermatitis (**Fig. 1b**).

We next sought to determine which of the two main DC populations in skin, epidermal LCs or dDCs, was essential for the elicitation of CHS. To deplete mice of all cutaneous DC subsets, we used mice with sequence expressing the diphtheria toxin receptor (DTR) under the control of the promoter of the gene encoding langerin as recipients (in such 'Langerin-DTR' mice, treatment with diphtheria toxin (DT) leads to depletion of langerin-positive cells) and mice that express a transgene encoding DTR under the control of promoter of the gene encoding CD11c as donors (in such 'CD11c-DTR' mice, treatment with DT leads to transient depletion of $CD11c^+$ DC populations). To selectively deplete mice of LCs or dDCs, we transferred bone marrow (BM) cells from C57BL/6 mice or CD11c-DTR mice into Langerin-DTR or C57BL/6 mice, respectively (**Supplementary Fig. 2a,b**). We injected DT into the chimeras to ensure depletion of each DC subset before elicitation and found that ear swelling and inflammatory histological findings were significantly attenuated in the absence of dDCs but not in the absence of LCs (**Fig. 1f** and **Supplementary Fig. 2c**). In addition, production of interferon-γ (IFN-γ) in skin T cells was substantially suppressed in mice depleted of dDCs (**Fig. 1g**). These results suggested that dDCs, not epidermal LCs, were essential for T cell activation and the elicitation of CHS responses.

Antigen-dependent proliferation of skin effector T cells *in situ*

To evaluate the effect of DC–T cell clusters in the dermis, we determined whether T cells had acquired the ability to proliferate via the accumulation of DC–T cell clusters in the dermis. We purified $CD4^+$ or $CD8^+$ T cells from the draining LNs of DNFB-sensitized mice, labeled

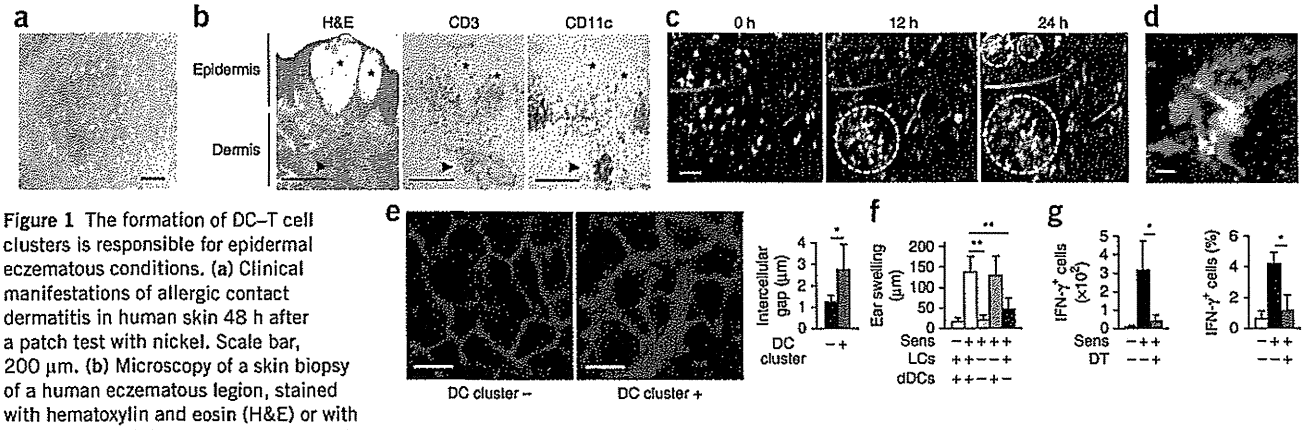

Figure 1 The formation of DC–T cell clusters is responsible for epidermal eczematous conditions. (a) Clinical manifestations of allergic contact dermatitis in human skin 48 h after a patch test with nickel. Scale bar, 200 μm. (b) Microscopy of a skin biopsy of a human eczematous legion, stained with hematoxylin and eosin (H&E) or with antibody to CD3 (anti-CD3) or anti-CD11c. *, epidermal vesicles; arrowheads indicate dDC–T cell clusters. Scale bars, 250 μm. (c) Sequential images of leukocyte clusters in the elicitation phase of CHS. White outlined areas indicate dermal accumulation of DCs (green) and T cells (red). Scale bar, 100 μm. (d) Enlargement of DC–T cell cluster in c. Scale bar, 10 μm. (e) Intercellular edema of the epidermis overlying a DC–T cell cluster in the dermis, with keratinocytes (red) visualized with isolectin B4 (left), and distance between adjacent keratinocytes above (+) or not above (–) a DC–T cell cluster ($n = 20$ images per condition) (right). Scale bars, 10 μm. (f) Ear swelling 24 h after CHS with (+) or without (–) sensitization (Sens) and with (–) or without (+) subset-specific depletion of DCs ($n = 5$ mice per group). (g) Quantification (left) and frequency (right) of IFN-γ-producing T cells in the ear 18 h after CHS with or without sensitization (as in f) and with (DT +) or without (DT –) depletion of dDCs ($n = 5$ mice per group). $^*P < 0.05$ and $^{**}P < 0.001$ (unpaired Student's *t*-test). Data are representative of five independent experiments (a–d) or three experiments (f,g) or are pooled from three experiments (e; error bars (e–g), s.d.).

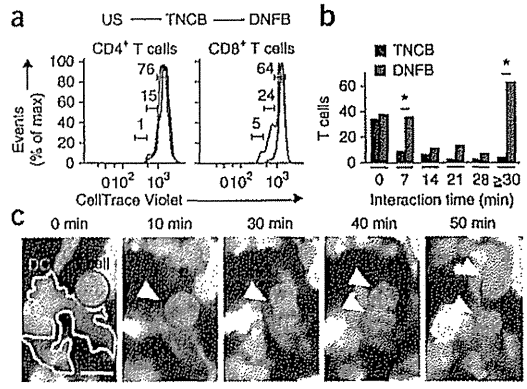

Figure 2 Antigen-dependent T cell proliferation in DC–T cell clusters. (a) Proliferation $CD4^+$ T cells (left) or $CD8^+$ T cells (right) in the skin of recipient mice 24 h after transfer of CellTrace Violet–labeled cells from donor mice left unsensitized (US) or sensitized with DNFB or TNCB, assessed as dilution of tracer in the challenged sites. Numbers adjacent to bracketed lines indicate percent cells that had proliferated. (b) Conjugation time of dDCs with T cells sensitized with DNFB ($n = 160$ T cells) or TNCB ($n = 60$ T cells), assessed at 24 h after challenge with DNFB. $^*P < 0.05$ (unpaired Student's t-test). (c) Sequential images of dividing T cells (red) in DC–T cell clusters. Green, dDCs; arrowheads indicate a dividing T cell. Data are representative of three experiments.

the cells with a division-tracking dye and transferred the cells into naive mice. Twenty-four hours after the application of DNFB to the recipient mice, we collected the skin to evaluate T cell proliferation by dilution of fluorescence intensity. Most of the infiltrating T cells (>90%) were $CD44^+CD62L^-$ effector T cells (**Supplementary Fig. 2d**). Among the infiltrating T cells, $CD8^+$ T cells proliferated actively, whereas the $CD4^+$ T cells showed low proliferative potency (**Fig. 2a**). This T cell proliferation was antigen dependent because T cells sensitized with the hapten TNCB (2,4,6-trinitrochlorobenzene) exhibited low proliferative activity in response to the application of DNFB (**Fig. 2a**). In line with that finding, the DC–T cell conjugation time was prolonged in the presence of the cognate antigen DNFB (**Fig. 2b**), and the T cells interacting with DCs within DC–T cell clusters proliferated (**Fig. 2c** and **Supplementary Movie 3**). These findings indicated that skin effector T cells conjugated with DCs and proliferated *in situ* in an antigen-dependent manner.

LFA-1-dependent activation of $CD8^+$ T cells in DC–T cell clusters

Sustained interaction between DCs and naive T cells, known as the 'immunological synapse', is maintained by cell adhesion molecules[10]. In particular, the integrin LFA-1 (CD58) on T cells binds to cell-surface glycoproteins, such as the intercellular adhesion molecule ICAM-1, on APCs, which is essential for the proliferation and activation of naive T cells during antigen recognition in the LNs. To determine whether LFA-1–ICAM-1 interactions are required for the activation of effector T cells in DC–T cell clusters in the skin, we elicited a CHS response in mouse ear skin with DNFB, then injected KBA, a neutralizing antibody to LFA-1, intravenously 14 h later. Such administration of KBA reduced the accumulation of T cells in the dermis (**Fig. 3a**). The velocity of T cells in the cluster was 0.65 ± 0.29 μm/min (mean ± s.d.) at 14 h after the DNFB challenge and increased up to threefold (1.64 ± 1.54 μm/min) at 8 h after treatment with KBA, while it was not affected by treatment with the isotype-matched control antibody immunoglobulin G (IgG) (**Fig. 3b**). At the outside of clusters, T cells smoothly migrated at the mean velocity of 2.95 ± 1.19 μm/min, consistent with published results[11], and this was not affected by treatment with the control antibody IgG (data not shown). Treatment with KBA also significantly attenuated ear swelling (**Fig. 3c**) as well as IFN-γ production by skin $CD8^+$ T cells (**Fig. 3d,e**). These results suggested that the DC–effector T cell conjugates were integrin dependent, similar to the DC–naive T cell interactions in draining LNs.

dDC clustering requires skin macrophages

We next examined the factors that initiated the accumulation of DC–T cell clusters. dDC clusters also formed in response to the initial application of hapten (sensitization phase), but their number decreased significantly 48 h after sensitization, while DC clusters persisted for 48 h in the elicitation phase (**Fig. 4a** and **Supplementary Fig. 3a**). These DC clusters were abrogated 7 d after application of DNFB (data not shown). These observations suggested that the accumulation of DC–T cell clusters was initiated by DC clustering, which then induced the accumulation, proliferation and activation of T cells, a process that depended on the presence of antigen-specific effector T cells *in situ*. DC clusters were also induced by solvents (such as acetone) or adjuvants (such as dibutylphthalic acid) and by pathogenic inoculation with *Mycobacterium bovis* bacillus Calmette-Guérin (**Supplementary Fig. 3b,c**). In addition, we observed DC clusters not only in the ear skin but also in other regions, such as the back skin and the footpad (**Supplementary Fig. 3d**). These results suggested that the formation of DC clusters was not an ear-specific event but was a general mechanism during skin inflammation.

The abundance of DC clusters in response to the application of DNFB was not altered in mice that lack T cells and B cells (recombinase

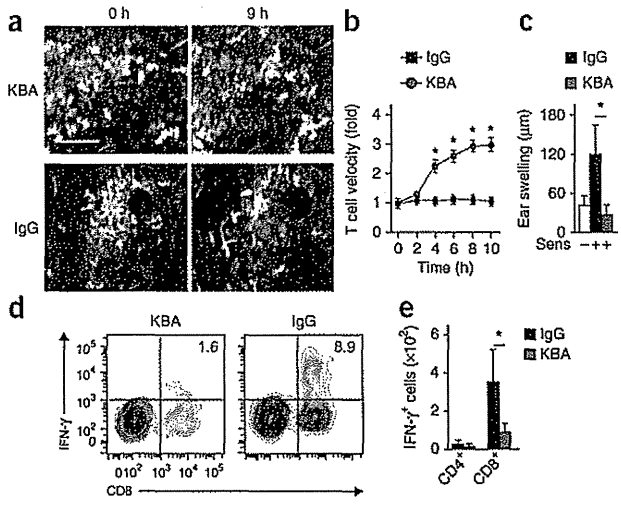

Figure 3 LFA-1 is essential for the persistence of DC–T cell clustering and for T cell activation in the skin. (a) Clusters of DCs (green) and T cells (red) in the DNFB-challenged site before (0 h) and 9 h after treatment with KBA (LFA-1-neutralizing antibody) or IgG (isotype-matched control antibody). Scale bar, 100 μm. (b) T cell velocity in DNFB-challenged sites at various times (horizontal axis) after treatment with KBA or IgG ($n = 30$ T cells per group), presented relative to velocity at time 0, set as 1. (c) Ear swelling 24 h after treatment with KBA or IgG in mice ($n = 5$ per group) left unsensitized (Sens –) or challenged with DNFB (Sens +). (d,e) IFN-γ production by $CD8^+$ T cells (d) and quantification of IFN-γ-producing cells in the $CD4^+$ or $CD8^+$ population (e) in skin from mice ($n = 5$ per group) challenged with DNFB, then treated with KBA or IgG 12 h later, assessed 6 h after antibody treatment. Numbers in top right quadrants (d) indicate percent IFN-γ$^+$CD8$^+$ T cells. $^*P < 0.05$ (unpaired Student's t-test). Data are representative of three experiments (error bars (b,c,e), s.d.).

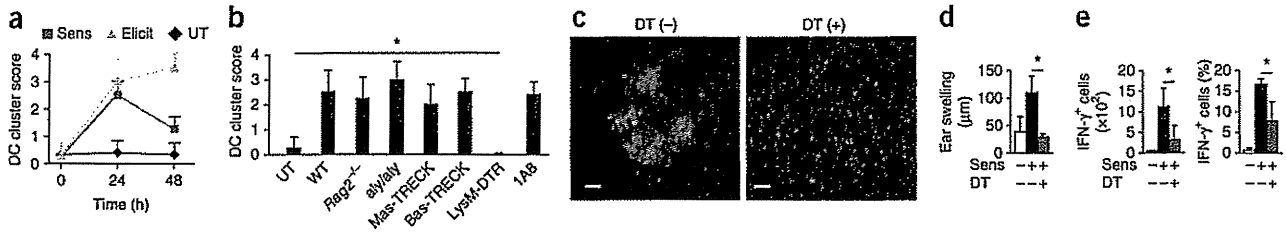

Figure 4 Macrophages are essential for DC cluster formation. (a) Score of DC cluster abundance in mice ($n = 4$ per group) left untreated (UT) or 24 h and 48 h after application of DNFB in the sensitization or elicitation phase of CHS; scores were assigned according to the size and number of clusters. (b) Score of DC cluster abundance (as in a) in untreated wild-type mice (UT), in DNFB-treated wild-type (C57BL/6) mice (WT), RAG-2-deficient mice (*Rag2*$^{-/-}$), aly/aly mice (aly/aly), DT-treated Mas-TRECK or Bas-TRECK mice or DT-treated C57BL/6 recipients of LysM-DTR BM cells, and in wild-type mice treated with 1A8 (anti-Ly6G) ($n = 4$ mice per group). (c) DC clusters in C57BL/6 chimeras given LysM-DTR BM with (right) or without (left) treatment of recipients with DT. Scale bars, 100 μm. (d) Ear swelling in C57BL/6 chimeras ($n = 5$ per group) given LysM-DTR BM with or without treatment with DT, assessed 24 h after no DNFB (Sense –) or application of DNFB to the recipients. (e) Quantification (left) and frequency (right) of IFN-γ-producing CD8$^+$ T cells in mice as in d ($n = 5$ per group). *$P < 0.05$ (unpaired Student's *t*-test). Data are representative of three (a,c,e), two (b) or four (d) experiments (error bars (b,d,e), s.d.).

RAG-2–deficient mice), in mice deficient in lymphoid tissue–inducer cells (alymphoblastic (aly/aly) mice)[12] or in mice depleted of mast cells or basophils (Mas-TRECK or Bas-TRECK mice treated with DT)[13,14] (**Fig. 4b**). In contrast, DC clustering was abrogated in C57BL/6 mice given transfer of BM from LysM-DTR mice (with sequence encoding a DTR cassette inserted into the gene encoding lysozyme M) followed by treatment of the recipients with DT to ensure depletion of both macrophages and neutrophils (**Fig. 4b,c**). Depletion of neutrophils alone, by administration of antibody 1A8 to Ly6G, did not interfere with the formation of DC clusters (**Fig. 4b**), which suggested that macrophages were required during the formation of DC clusters, but neutrophils were not. Of note, the formation of DC clusters was not attenuated by treatment with the LFA-1-neutralizing antibody KBA (**Supplementary Fig. 3e,f**), which suggested that macrophage-DC interactions were LFA-1 independent. Consistent with the formation of DC clusters, elicitation of the CHS response (**Fig. 4d**) and IFN-γ production by skin T cells (**Fig. 4e**) were significantly suppressed in chimeras given LysM-DTR BM and treated with DT. Thus, skin macrophages were required for the formation of DC clusters, which was necessary for T cell activation and the elicitation of CHS.

Perivascular DCs clustering requires macrophages

To examine the migratory kinetics of dermal macrophages and DCs *in vivo*, we visualized them by two-photon microscopy. *In vivo* labeling of blood vessels with dextran conjugated to the hydrophobic red fluorescent dye TRITC (tetramethylrhodamine isothiocyanate) revealed that dDCs distributed diffusely in the steady state (**Fig. 5a**, left). After application of DNFB to the ears of mice previously sensitized with DNFB, dDCs accumulated mainly around post-capillary venules (**Fig. 5a**, right, and **b**). Time-lapse imaging revealed that some dDCs showed directional migration toward TRITC$^+$ cells that were labeled red by incorporation of extravasated TRITC-dextran (**Fig. 5c** and **Supplementary Movie 4**). Most of the TRITC$^+$ cells were F4/80$^+$CD11b$^+$ macrophages (**Supplementary Fig. 4a**). These observations prompted us to investigate the role of macrophages in DC accumulation. We used a chemotaxis assay to determine whether macrophages attracted the DCs. We isolated dDCs and dermal macrophages from dermal skin cell suspensions and incubated them for 12 h in a Transwell assay. dDCs placed in the upper wells migrated efficiently to lower wells that contained dermal macrophages (**Fig. 5d**). However, we did not observe such dDC migration when macrophages were absent from the lower wells (**Fig. 5d**). Thus, dermal macrophages were able to attract dDCs *in vitro*, which may have led to the accumulation of dDCs around post-capillary venules.

DC cluster formation requires IL-1α upon antigen challenge

We attempted to explore the mechanism underlying the formation of DC clusters. We observed that DC accumulation occurred during the first application of hapten (**Fig. 4a**), which suggested that an antigen-nonspecific mechanism, such as production of the proinflammatory mediator IL-1, may initiate DC clustering. DNFB-induced accumulation of DCs was not suppressed in mice deficient in NLRP3 or deficient in caspase-1 and caspase-11 more than their wild-type counterparts, but it was significantly lower in IL-1R1-deficient mice (which lack the receptor for IL-1α and IL-1β and for the IL-1 receptor antagonist (IL-1ra)) than in their wild-type counterparts, as well as after the subcutaneous administration of IL-1ra than before treatment with the antagonist (**Fig. 6a,b**). Consistent with those observations, the elicitation of CHS and IFN-γ production by skin T cells were significantly attenuated in mice that lacked both IL-1α and IL-1β (**Fig. 6c,d**). In addition, the formation of dDC clusters was suppressed significantly by the subcutaneous injection of a neutralizing antibody to IL-1α but

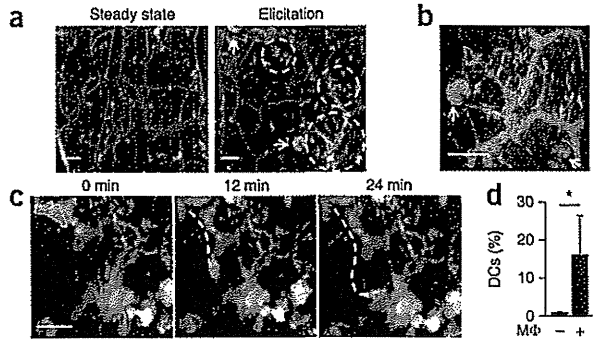

Figure 5 Macrophages mediate the perivascular formation of DC clusters. (a) Distribution of dDCs (green) in the steady state (left) and in the elicitation phase of CHS (right). White outlined areas indicate DC clusters; arrows indicate sebaceous glands visualized with BODIPY (green); yellow and red, blood vessels; red, macrophages. Scale bars, 100 μm. (b) Enlargement of a perivascular DC cluster. Arrows indicate sebaceous glands of hair follicles. Scale bar, 100 μm.(c) Sequential images of dDCs (green) and macrophages (red) in the elicitation phase of CHS. White dashed line represents the track of a DC. Scale bar, 30 μm. (d) Chemotaxis of dDCs in the presence (+) or absence (–) of macrophages (MΦ) prepared from ear skin, presented as the frequency of dDCs that transmigrated into the lower chamber of a Transwell (relative to input dDCs). *$P < 0.05$ (unpaired Student's *t*-test). Data are representative of three experiments (error bars (d), s.d.).

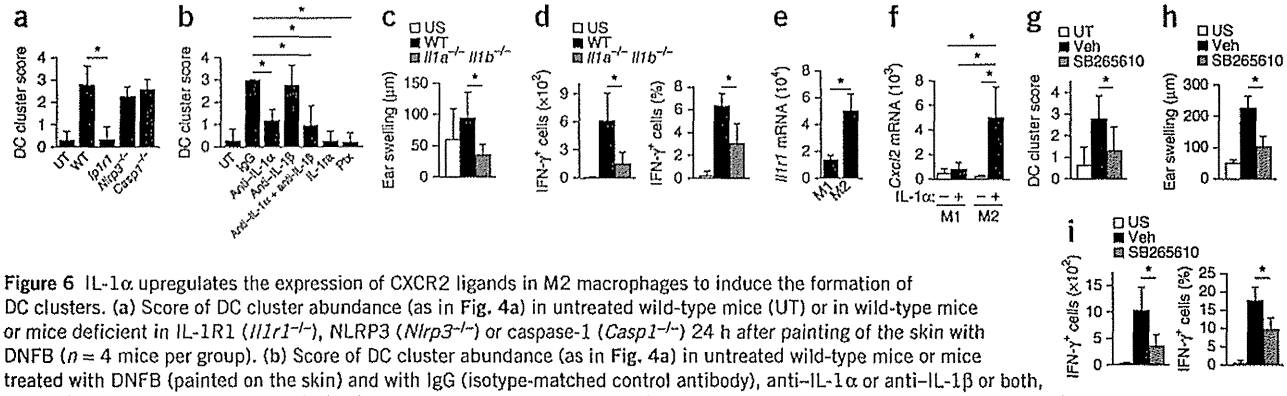

Figure 6 IL-1α upregulates the expression of CXCR2 ligands in M2 macrophages to induce the formation of DC clusters. (a) Score of DC cluster abundance (as in Fig. 4a) in untreated wild-type mice (UT) or in wild-type mice or mice deficient in IL-1R1 (*Il1r1*$^{-/-}$), NLRP3 (*Nlrp3*$^{-/-}$) or caspase-1 (*Casp1*$^{-/-}$) 24 h after painting of the skin with DNFB ($n = 4$ mice per group). (b) Score of DC cluster abundance (as in Fig. 4a) in untreated wild-type mice or mice treated with DNFB (painted on the skin) and with IgG (isotype-matched control antibody), anti–IL-1α or anti–IL-1β or both, recombinant IL-1ra or pertussis toxin (Ptx), assessed 24 h after treatment with hapten ($n = 4$ mice per group). (c,d) Ear swelling 24 h after application of DNFB (c) and quantification (d, left) and frequency (d, right) of IFN-γ-producing CD8$^+$ T cells in the ear 18 h after application of DNFB (d) in unsensitized wild-type mice (US) or in mice lacking both IL-1α and IL-1β (*Il1a*$^{-/-}$*Il1b*$^{-/-}$) and wild-type mice given adoptive transfer of DNFB-sensitized T cells ($n = 5$ mice per group). (e) Quantitative RT-PCR analysis of *Il1r1* mRNA in M1 or M2 macrophages ($n = 4$ mice per group). (f) Quantitative RT-PCR analysis of *Cxcl2* mRNA in M1 or M2 macrophages cultured with (+) or without (–) IL-1α. (g) Score of DC cluster abundance (as in Fig. 4a) in untreated wild-type mice (UT) or in mice treated with DNFB (painted on the skin) in the presence (SB265610) or absence (vehicle (Veh)) of a CXCR2 inhibitor, assessed 24 h after treatment with DNFB ($n = 4$ mice per group). (h,i) Ear swelling 24 h after application of DNFB (h) and quantification (i, right) and frequency (i, left) of IFN-γ-producing CD8$^+$ T cells 18 h after application of DNFB (i) in unsensitized wild-type mice (US) or in mice treated with DNFB in the presence or absence of the CXCR2 inhibitor SB265610 ($n = 5$ mice per group). *$P < 0.05$ (unpaired Student's *t*-test). Data are representative of two (a,c,d) or three (b,e–i) experiments (error bars, s.d.).

was suppressed only marginally by a neutralizing antibody to IL-1β (**Fig. 6b**). Because keratinocytes are known to produce IL-1α upon application of a hapten[15], our results suggested a major role for IL-1α in mediating the formation of DC clustering.

M2 macrophages produce chemokine CXCL2 to attract dDCs

To further characterize how macrophages attract dDCs, we examined expression of the gene encoding IL-1Rα (*Il1r1*) in BM-derived classically activated (M1) and alternatively activated (M2) macrophages, classified as such on the basis of differences in the expression of *Tnf*, *Nos2*, *Il12a*, *Arg1*, *Retnla* and *Chi313* mRNA[16] (**Supplementary Fig. 4b**). We found that M2 macrophages had higher expression of *Il1r1* mRNA than did M1 macrophages (**Fig. 6e**). We also found that subcutaneous injection of pertussis toxin, an inhibitor specific for inhibitory regulative G protein, almost completely abrogated the formation of DC clusters in response to hapten stimuli (**Fig. 6b**), which suggested that signaling through chemokines coupled to the inhibitory regulative G protein was required for the formation of DC clusters.

We next used microarray analysis to examine the effect of IL-1α on the expression of chemokine-encoding genes in M1 and M2 macrophages. Treatment with IL-1α did not enhance such expression in M1 macrophages, whereas it increased the expression of *Ccl5*, *Ccl17*, *Ccl22* and *Cxcl2* mRNA in M2 macrophages (**Supplementary Table 1**). Among those, *Cxcl2* mRNA expression was enhanced most prominently by treatment with IL-1α, a result we confirmed by real-time PCR analysis (**Fig. 6f**). Consistently, *Cxcl2* mRNA expression was much higher in DNFB-painted skin than in untreated skin (**Supplementary Fig. 5a**) and was not affected by neutrophil depletion with the 1A8 antibody to Ly6G (**Supplementary Fig. 5b,c**). In addition, IL-1α-treated dermal macrophages produced *Cxcl2* mRNA *in vitro* (**Supplementary Fig. 5d**). These results suggested that dermal macrophages, but not neutrophils, were the main source of CXCL2 during CHS. We also detected high expression of *Cxcr2* mRNA (which encodes the receptor for CXCL2) in DCs (**Supplementary Fig. 5e**); this prompted us to examine the role of CXCR2 in dDCs. The formation of DC clusters in response to DNFB was substantially reduced by intraperitoneal administration of the CXCR2 inhibitor SB265610 (ref. 17) (**Fig. 6g**). In addition, treatment with SB265610 during the elicitation of CHS with DNFB inhibited ear swelling (**Fig. 6h**) and IFN-γ production by skin T cells (**Fig. 6i**).

Together our results indicated that in the absence of effector T cells specific for a cognate antigen (i.e., in the sensitization phase of CHS), DC clustering was a transient event, and hapten-carrying DCs migrated into draining LNs to establish sensitization. On the other hand, in the presence of the antigen and antigen-specific effector or memory T cells, DC clustering was followed by accumulation of T cells (i.e., in the elicitation phase of CHS) (**Supplementary Fig. 6**). Thus, dermal macrophages were essential for initiating the formation of DC clusters through the production of CXCL2, and DC clustering had a role in the efficient activation of skin T cells.

DISCUSSION

Although the mechanistic events in the sensitization phase in cutaneous immunity have been studied thoroughly over 20 years[18,19], the types of immunological events that occur during the elicitation phases in the skin has remained unclear. Here we have described the antigen-dependent induction of DC–T cell clusters in the skin in a mouse model of CHS and showed that DC–effector T cell interactions in these clusters were required for the induction of efficient antigen-specific immune responses in the skin. We found that dDCs, but not epidermal LCs, were essential for the presentation of antigen to skin effector T cells and that they exhibited sustained association with effector T cells in an antigen- and LFA-1-dependent manner. IL-1α, not the inflammasome, initiated the formation of these perivascular DC clusters.

Epidermal contact with antigens triggers the release of IL-1 in the skin[15]. Published studies have shown that the epidermal keratinocytes constitute a major reservoir of IL-1α[6] and that mechanical stress applied to keratinocytes permits the release of large amounts of IL-1α even in the absence of cell death[20]. The cellular source of IL-1α in this process remains unclear. We found that IL-1α activated macrophages that subsequently attracted dDCs, mainly to areas around post-capillary venules, where effector T cells are known to transmigrate from the blood into the skin[21]. In the presence of the antigen and antigen-specific

effector T cells, DC clustering was followed by T cell accumulation. Therefore, we propose that these perivascular dDC clusters may provide antigen-presentation sites for efficient activation of effector T cells. This is suggested by the observations that CHS responses and intracutaneous T cell activation were attenuated substantially in the absence of these clusters, in conditions of macrophage depletion or inhibition of integrin function, IL-1R signaling[22,23] or CXCR2 signaling[24].

In contrast to antigen presentation in the skin, antigen presentation in other peripheral barrier tissues is relatively well understood. In submucosal areas, specific sentinel lymphoid structures (mucosa-associated lymphoid tissue (MALT)) serve as peripheral antigen-presentation sites[25], and lymphoid follicles are present in non-inflammatory bronchi (bronchus-associated lymphoid tissue (BALT)). These structures serve as antigen-presentation sites in nonlymphoid peripheral organs. By analogy, the concept of skin-associated lymphoid tissue (SALT) was proposed in the early 1980s, on the basis of findings that cells in the skin are able to capture, process and present antigens[26,27]. However, the role of cellular skin components as antigen-presentation sites has remained uncertain. Here we have identified an inducible structure formed by dermal macrophages, dDCs and effector T cells, which seemed to accumulate sequentially. Because formation of this structure was essential for efficient activation of effector T cells, these inducible leukocyte clusters may function as SALTs. Unlike leukocyte clusters in MALT, these leukocyte clusters were not found in the steady state but were induced during the development of an adaptive immune response. Therefore, these clusters might be better called 'inducible SALTs', similar to inducible BALTs in the lung[28]. In contrast to the cells present in inducible BALT, we did not identify naive T cells or B cells in SALT (data not shown), which suggested that the leukocyte clusters in the skin may be specialized for the activation of effector T cells but not for the activation of naive T cells. Our findings suggest that approaches for the selective inhibition of this structure may have novel therapeutic benefit in inflammatory disorders of the skin.

METHODS

Methods and any associated references are available in the online version of the paper.

Accession codes. GEO: microarray data, GSE53680.

Note: Any Supplementary Information and Source Data files are available in the online version of the paper.

ACKNOWLEDGMENTS

We thank H. Yagita (Juntendo University) for the KBA neutralizing antibody to LFA-1; P. Bergstresser and J. Cyster for critical reading of our manuscript. Supported by grants-in-aid for Scientific Research from the Ministry of Education, Culture, Sports, Science and Technology of Japan.

AUTHOR CONTRIBUTIONS

Y.N., G.E. and K.K. designed this study and wrote the manuscript; Y.N., G.E., S. Nakamizo, S.O., S.H., N.K., A.O., A.K., T. Honda and S. Nakajima performed the experiments and analyzed data; S.T. and Y.S. did experiments related to microarray analysis; K.J.I., H.T., H.Y., Y.I., M.K. and L.g.N. developed experimental reagents and gene-targeted mice; J.F. and E.G.-Y. did experiments related to immunohistochemistry of human samples; T.O., T. Hashimoto, Y.M. and K.K. directed the project and edited the manuscript; and all authors reviewed and discussed the manuscript.

COMPETING FINANCIAL INTERESTS

The authors declare no competing financial interests.

1. von Andrian, U.H. & Mempel, T.R. Homing and cellular traffic in lymph nodes. *Nat. Rev. Immunol.* **3**, 867–878 (2003).
2. Clark, R.A. *et al.* The vast majority of CLA+ T cells are resident in normal skin. *J. Immunol.* **176**, 4431–4439 (2006).
3. Wang, L. *et al.* Langerin expressing cells promote skin immune responses under defined conditions. *J. Immunol.* **180**, 4722–4727 (2008).
4. Tuckermann, J.P. *et al.* Macrophages and neutrophils are the targets for immune suppression by glucocorticoids in contact allergy. *J. Clin. Invest.* **117**, 1381–1390 (2007).
5. Sims, J.E. & Smith, D.E. The IL-1 family: regulators of immunity. *Nat. Rev. Immunol.* **10**, 89–102 (2010).
6. Murphy, J.E., Robert, C. & Kupper, T.S. Interleukin-1 and cutaneous inflammation: a crucial link between innate and acquired immunity. *J. Invest. Dermatol.* **114**, 602–608 (2000).
7. Nakae, S. *et al.* IL-1-induced tumor necrosis factor-α elicits inflammatory cell infiltration in the skin by inducing IFN-γ-inducible protein 10 in the elicitation phase of the contact hypersensitivity response. *Int. Immunol.* **15**, 251–260 (2003).
8. Thyssen, J.P., Linneberg, A., Menne, T., Nielsen, N.H. & Johansen, J.D. Contact allergy to allergens of the TRUE-test (panels 1 and 2) has decreased modestly in the general population. *Br. J. Dermatol.* **161**, 1124–1129 (2009).
9. Ng, L.G. *et al.* Migratory dermal dendritic cells act as rapid sensors of protozoan parasites. *Plos Pathog* **4**, e1000222 (2008).
10. Springer, T.A. & Dustin, M.L. Integrin inside-out signaling and the immunological synapse. *Curr. Opin. Cell Biol.* **24**, 107–115 (2012).
11. Egawa, G. *et al. In vivo* imaging of T-cell motility in the elicitation phase of contact hypersensitivity using two-photon microscopy. *J. Invest. Dermatol.* **131**, 977–979 (2011).
12. Miyawaki, S. *et al.* A new mutation, aly, that induces a generalized lack of lymph nodes accompanied by immunodeficiency in mice. *Eur. J. Immunol.* **24**, 429–434 (1994).
13. Sawaguchi, M. *et al.* Role of mast cells and basophils in IgE responses and in allergic airway hyperresponsiveness. *J. Immunol.* **188**, 1809–1818 (2012).
14. Otsuka, A. *et al.* Requirement of interaction between mast cells and skin dendritic cells to establish contact hypersensitivity. *PLoS ONE* **6**, e25538 (2011).
15. Enk, A.H. & Katz, S.I. Early molecular events in the induction phase of contact sensitivity. *Proc. Natl. Acad. Sci. USA* **89**, 1398–1402 (1992).
16. Weisser, S.B., McLarren, K.W., Kuroda, E. & Sly, L.M. Generation and characterization of murine alternatively activated macrophages. *Methods Mol. Biol.* **946**, 225–239 (2013).
17. Liao, L. *et al.* CXCR2 blockade reduces radical formation in hyperoxia-exposed newborn rat lung. *Pediatr. Res.* **60**, 299–303 (2006).
18. Honda, T., Egawa, G., Grabbe, S. & Kabashima, K. Update of immune events in the murine contact hypersensitivity model: toward the understanding of allergic contact dermatitis. *J. Invest. Dermatol.* **133**, 303–315 (2013).
19. Kaplan, D.H., Igyarto, B.Z. & Gaspari, A.A. Early immune events in the induction of allergic contact dermatitis. *Nat. Rev. Immunol.* **12**, 114–124 (2012).
20. Lee, R.T. *et al.* Mechanical deformation promotes secretion of IL-1 alpha and IL-1 receptor antagonist. *J. Immunol.* **159**, 5084–5088 (1997).
21. Sackstein, R., Falanga, V., Streilein, J.W. & Chin, Y.H. Lymphocyte adhesion to psoriatic dermal endothelium is mediated by a tissue-specific receptor/ligand interaction. *J. Invest. Dermatol.* **91**, 423–428 (1988).
22. Kish, D.D., Gorbachev, A.V. & Fairchild, R.L. IL-1 receptor signaling is required at multiple stages of sensitization and elicitation of the contact hypersensitivity response. *J. Immunol.* **188**, 1761–1771 (2012).
23. Kondo, S. *et al.* Interleukin-1 receptor antagonist suppresses contact hypersensitivity. *J. Invest. Dermatol.* **105**, 334–338 (1995).
24. Cattani, F. *et al.* The role of CXCR2 activity in the contact hypersensitivity response in mice. *Eur. Cytokine Netw.* **17**, 42–48 (2006).
25. Brandtzaeg, P., Kiyono, H., Pabst, R. & Russell, M.W. Terminology: nomenclature of mucosa-associated lymphoid tissue. *Mucosal Immunol.* **1**, 31–37 (2008).
26. Streilein, J.W. Skin-associated lymphoid tissues (SALT): origins and functions. *J. Invest. Dermatol.* **80** (suppl.), 12s–16s (1983).
27. Egawa, G. & Kabashima, K. Skin as a peripheral lymphoid organ: revisiting the concept of skin-associated lymphoid tissues. *J. Invest. Dermatol.* **131**, 2178–2185 (2011).
28. Moyron-Quiroz, J.E. *et al.* Role of inducible bronchus associated lymphoid tissue (iBALT) in respiratory immunity. *Nat. Med.* **10**, 927–934 (2004).

ONLINE METHODS

Mice. 8- to 12-week-old female C57BL/6 mice were used in this study. C57BL/6N mice were from SLC. Langerin-eGFP-DTR mice[29], CD11c-DTR mice[30], CD11c-YFP mice (that express CD11c tagged with YFP)[31], LysM-DTR mice[32], RAG-2-deficient mice[33], Mas-TRECK mice[13,14], Bas-TRECK mice[13,14], ALY/NscJcl- aly/aly mice[12], IL-1α/β-deficient mice[34], IL-1R1-deficient mice[35], NLRP3-deficient mice[36] and caspase-1/11-deficient mice[37] have been described. All experimental procedures were approved by the Institutional Animal Care and Use Committee of Kyoto University Graduate School of Medicine.

Human subjects. Biopsy samples of human skin were obtained from a nickel-reactive patch after 48 h after placement of nickel patch tests in patients with previously proven allergic contact dermatitis. A biopsy of petrolatum-occluded skin was also obtained as a control. Informed consent was obtained under protocols approved by the Institutional Review Board at the Icahn School of Medicine at Mount Sinai School Medical Center, and the Rockefeller University in New York.

Induction of CHS responses. Mice were sensitized on shaved abdominal skin with 25 μl 0.5% (wt/vol) DNFB (1-fluoro-2,4-dinitrofluorobenzene ; Nacalai Tesque) dissolved in acetone and olive oil (at a ratio of 4:1). Five days later, the ears were challenged with 20 μl 0.3% DNFB. For adoptive transfer, T cells were magnetically sorted, with an autoMACS (Miltenyi Biotec), from the draining LNs of sensitized mice and then were transferred intravenously (1×10^7 cells) into naive mice.

Depletion of cutaneous DC subsets, macrophages and neutrophils. For depletion of all cutaneous DC subsets (including LCs), 6-week-old Langerin-DTR mice were irradiated (two doses of 550 rads given 3 h apart) and were given transfer of 1×10^7 BM cells from CD11c-DTR mice. Eight weeks later, 2 μg DT (Sigma-Aldrich) was injected intraperitoneally. For selective depletion of LCs, irradiated Langerin-DTR mice were given transfer of BM cells from C57BL/6 mice, and 1 μg DT was injected. For selective depletion of dDCs, irradiated C57BL/6 mice were given transfer of BM cells from CD11c-DTR mice, and 2 μg DT was injected. For depletion of macrophages, irradiated C57BL/6 mice were given transfer of BM cells from LysM-DTR mice and 800 ng DT was injected. For depletion of neutrophils, anti-Ly6G (1A8; BioXCell) was administered to mice intravenously at a dose of 0.5 mg per mouse 24 h before experiments.

Time-lapse imaging of cutaneous DCs, macrophages and T cells. Cutaneous DCs were observed in CD11c-YFP mice. For labeling of cutaneous macrophages *in vivo*, 5 mg TRITC-dextran (Sigma-Aldrich) was injected intravenously and mice were allowed to 'rest' for 24 h. At that time, cutaneous macrophages became fluorescent because they had incorporated extravasated dextran. For labeling of skin-infiltrating T cells, T cells from DNFB-sensitized mice were labeled with CellTracker Orange (CMTMR (5-(and-6)-(((4-chloromethyl)benzoyl) amino)tetramethylrhodamine); Invitrogen) and were adoptively transferred into recipient mice. Keratinocytes and sebaceous glands were visualized by subcutaneous injection of isolectin B4 (Invitrogen) and BODIPY (Molecular Probes), respectively. Mice were positioned on a heating plate on the stage of a two-photon IX-81 microscope (Olympus) and their ear lobes were fixed beneath a cover slip with a single drop of immersion oil. Stacks of ten images, spaced 3 μm apart, were acquired at intervals of 1–7 min for up to 24 h. For calculation of T cell and DC velocities, movies were processed and analyzed with Imaris 7.2.1 software (Bitplane).

Histology and immunohistochemistry. For histological examination, tissues were fixed with 10% formalin in phosphate-buffered saline, then were embedded in paraffin. Sections with a thickness of 5 μm were prepared and then were stained with hematoxylin and eosin. For whole-mount staining, the ears were split into dorsal and ventral halves and were incubated for 30 min at 37 °C with 0.5 M ammonium thiocyanate. Then the dermal sheets were separated and fixed in acetone for 10 min at −20 °C. After treatment with Image-iT FX Signal Enhancer (Invitrogen), the sheets were incubated with antibody to mouse MHC class II (M5/114.15.2; eBioscience) followed by incubation with antibody to rat IgG conjugated to Alexa Fluor 488 (A-11006; Invitrogen) or Alexa Fluor 594 (A-11007; Invitrogen). The slides were mounted with a ProLong Antifade kit with the DNA-binding dye DAPI (4′6-diamidino-2-phenylindole; Molecular Probes) and were observed with a fluorescent microscope (BZ-900; KEYENCE). The number and size of DC clusters were evaluated in ten fields of 1 mm^2 per ear and were assigned scores according to the criteria in **Supplementary Figure 5a**.

Cell isolation and flow cytometry. For the isolation of skin lymphocytes, the split ears were incubated for 1 h at 37 °C in digestion buffer (RPMI medium supplemented with 2% FCS, 0.33 mg/ml of Liberase TL (Roche) and 0.05% DNase I (Sigma-Aldrich)). After that incubation, the tissues were disrupted by passage through a 70-μm cell strainer and stained with the appropriate antibodies (identified below). For analysis of intracellular cytokine production, cell suspensions were obtained in the presence of 10 μg/ml of brefeldin A (Sigma-Aldrich) and were fixed with Cytofix Buffer and permeabilized with Perm/Wash Buffer according to the manufacturer's protocol (BD Biosciences). Cells were stained with the following: antibody to mouse CD4 (GK1.5), anti-CD8 (53-6.7), anti-CD11b (M1/70), anti-CD11c (N418), anti-B220 (RA3-6B2), antibody to MHC class II (M5/114.15.2), anti-F4/80 (BM8), anti-IFN-γ (XMG1.2), anti-Gr1 (RB6-8c5) and 7-amino-actinomycin D (all from eBioscience); anti-mouse CD45 (30-F11) and anti-TCR-β (H57-597; both from BioLegend); and anti-CD16-CD32 (2.4G2; BD Biosciences). Flow cytometry was done with an LSR Fortessa (BD Biosciences) and data were analyzed with FlowJo software (TreeStarA).

Chemotaxis assays. Chemotaxis was assessed as described with some modifications[38]. The dermis of the ear skin was minced and then was digested for 30 min at 37 °C with 2 mg/ml collagenase type II (Worthington Biochemical) containing 1 mg/ml hyaluronidase (Sigma-Aldrich) and 100 μg/ml DNase I (Sigma-Aldrich). DDCs and macrophages were isolated with an autoMACS. Alternatively, BM-derived DCs and macrophages were prepared. 1×10^6 DCs were added to a Transwell insert with a pore size of 5 μm (Corning), and 5×10^5 macrophages were added to the lower wells, and the cells were incubated for 12 h at 37 °C. A known number of fluorescent reference beads (FlowCount fluorospheres; Beckman Coulter) were added to each sample to allow accurate quantification of cells that had migrated to the lower wells by flow cytometry.

Cell proliferation assay. Mice were sensitized with 25 μl 0.5% DNFB or 7% trinitrochlorobenzene (Chemical Industry). Five days later, T cells were magnetically separated from the draining LNs of each group of mice and were labeled with CellTrace Violet according to the manufacturer's protocol (Invitrogen). 1×10^6 T cells were adoptively transferred into naive mice, and the ears of the recipient mice were challenged with 20 μl of 0.5% DNFB. 24 h later, ears were collected and analyzed by flow cytometry.

***In vitro* differentiation of DCs and M1 and M2 macrophages from BM cells.** BM cells from the tibias and fibulas were plated at a density of 5×10^6 cells per 10-cm dish on day 0. For DC differentiation, cells were cultured at 37 °C in 5% CO_2 in cRPMI medium (RPMI medium supplemented with 1% L-glutamine, 1% HEPES, 0.1% 2-mercaptoethanol and 10% FBS) containing 10 ng/ml granulocyte-macrophage colony-stimulating factor (Peprotech). For macrophage differentiation, BM cells were cultured in cRPMI medium containing 10 ng/ml macrophage colony-stimulating factor (Peprotech). The medium was replaced on days 3 and 6 and cells were harvested on day 9. For the induction of M1 macrophages or M2 macrophages, cells were stimulated for 48 h with IFN-γ (10 ng/ml; R&D Systems) or with IL-4 (20 ng/ml; R&D Systems), respectively.

***In vitro* IL-1α-stimulation assay of dermal macrophages.** Dermal macrophages were separated from mice deficient in IL-1α and IL-1β[34] to avoid preactivation during cell preparations. Split ears were treated for 30 min at 37 °C with 0.25% trypsin and EDTA for removal of the epidermis, then were minced and then incubated with collagenase as described above. $CD11b^+$ cells were separated by magnetic-activated cell sorting, and 2×10^5 cells per well in 96-well plates were incubated for 24 h with or without 10 ng/ml IL-1α (R&D Systems).

doi:10.1038/ni.2992

Blocking assay. For the LFA-1-blocking assay, mice were given intravenous injection of 100 μg KBA (neutralizing antibody to LFA-1; a gift from H. Yagita) 12–14 h after challenge with 20 μl 0.5% DNFB. For blockade of IL-1R, mice were given subcutaneous injection of 10 μg recombinant mouse IL-1ra (PROSPEC) 5 h before challenge. For blockade of CXCR2, mice were given intraperitoneal treatment with 50 μg CXCR2 inhibitor[17] (SB265610; Tocris Bioscience) 6 h before and at the time of painting of the skin with hapten.

Quantitative PCR analysis. Total RNA was isolated with an RNeasy Mini kit (Qiagen, Hilden, Germany). cDNA was synthesized with a PrimeScript RT reagent kit and random hexamers according to the manufacturer's protocol (TaKaRa). A LightCycler 480 and LightCycler SYBR Green I Master mix were used according to the manufacturer's protocol (Roche) for quantitative PCR (primer sequences, **Supplementary Table 2**). The expression of each gene was normalized to that of the control gene *Gapdh*.

Microarray analysis. Total RNA was isolated with an RNeasy Mini Kit according to the manufacturer's protocol (Qiagen). An amplified sense-strand DNA product was synthesized with the Ambion WT Expression Kit (Life Technologies), was fragmented and labeled by the WT Terminal Labeling and Controls Kit (Affymetrix) and was hybridized to a Mouse Gene 1.0 ST Array (Affymetrix). We used the robust multiarray average algorithm for log transformation ($\log_2$) and normalization of the GeneChip data.

General experimental design and statistical analysis. For animal experiments, a sample size of three to five mice per group was used on the basis of past experience in generating statistical significance. Mice were randomly assigned to study groups and no specific randomization or blinding protocol was used. Sample or mouse identity was not masked for any of these studies. Prism software (GraphPad) was used for statistical analyses. Normal distribution was assumed a priori for all samples. Unless indicated otherwise, an unpaired parametric *t*-test was used for comparison of data sets. In cases in which the data-point distribution was not Gaussian, a nonparametric *t*-test was also applied. *P* values of less than 0.05 were considered significant.

29. Kissenpfennig, A. *et al.* Dynamics and function of Langerhans cells *in vivo*: dermal dendritic cells colonize lymph node areas distinct from slower migrating Langerhans cells. *Immunity* **22**, 643–654 (2005).
30. Jung, S. *et al. In vivo* depletion of CD11c$^+$ dendritic cells abrogates priming of CD8$^+$ T cells by exogenous cell-associated antigens. *Immunity* **17**, 211–220 (2002).
31. Lindquist, R.L. *et al.* Visualizing dendritic cell networks *in vivo*. *Nat. Immunol.* **5**, 1243–1250 (2004).
32. Miyake, Y. *et al.* Protective role of macrophages in noninflammatory lung injury caused by selective ablation of alveolar epithelial type II Cells. *J. Immunol.* **178**, 5001–5009 (2007).
33. Hao, Z. & Rajewsky, K. Homeostasis of peripheral B cells in the absence of B cell influx from the bone marrow. *J. Exp. Med.* **194**, 1151–1164 (2001).
34. Horai, R. *et al.* Production of mice deficient in genes for interleukin (IL)-1α, IL-1β, IL-1α/β, and IL-1 receptor antagonist shows that IL-1β is crucial in turpentine-induced fever development and glucocorticoid secretion. *J. Exp. Med.* **187**, 1463–1475 (1998).
35. Coban, C. *et al.* Immunogenicity of whole-parasite vaccines against *Plasmodium falciparum* involves malarial hemozoin and host TLR9. *Cell Host Microbe* **7**, 50–61 (2010).
36. Martinon, F., Petrilli, V., Mayor, A., Tardivel, A. & Tschopp, J. Gout-associated uric acid crystals activate the NALP3 inflammasome. *Nature* **440**, 237–241 (2006).
37. Koedel, U. *et al.* Role of caspase-1 in experimental pneumococcal meningitis: evidence from pharmacologic caspase inhibition and caspase-1-deficient mice. *Ann. Neurol.* **51**, 319–329 (2002).
38. Tomura, M. *et al.* Activated regulatory T cells are the major T cell type emigrating from the skin during a cutaneous immune response in mice. *J. Clin. Invest.* **120**, 883–893 (2010).

Basophils regulate the recruitment of eosinophils in a murine model of irritant contact dermatitis

Chisa Nakashima, MD,[a] Atsushi Otsuka, MD, PhD,[a] Akihiko Kitoh, MD, PhD,[a] Tetsuya Honda, MD, PhD,[a] Gyohei Egawa, MD, PhD,[a] Saeko Nakajima, MD, PhD,[a] Satoshi Nakamizo, MD,[a] Makoto Arita, PhD,[b] Masato Kubo, PhD,[c,d] Yoshiki Miyachi, MD, PhD,[a] and Kenji Kabashima, MD, PhD[a] *Kyoto, Tokyo, Kanagawa, and Chiba, Japan*

Background: Although eosinophils have been detected in several human skin diseases in the vicinity of basophils, how eosinophils infiltrate the skin and the role of eosinophils in the development of skin inflammation have yet to be examined.

Objective: Using murine irritant contact dermatitis (ICD) as a model, we sought to clarify the roles of eosinophils in ICD and the underlying mechanism of eosinophil infiltration of the skin.

Methods: We induced croton oil–induced ICD in eosinophil-deficient ΔdblGATA mice with or without a reactive oxygen species (ROS) inhibitor. We performed cocultivation with fibroblasts and bone marrow–derived basophils and evaluated eosinophil migration using a chemotaxis assay.

Results: ICD responses were significantly attenuated in the absence of eosinophils or by treatment with the ROS inhibitor. ROS was produced abundantly by eosinophils, and both basophils and eosinophils were detected in human and murine ICD skin lesions. In coculture experiments, basophils attracted eosinophils, especially in the presence of fibroblasts. Moreover, basophils produced IL-4 and TNF-α in contact with fibroblasts and promoted the expression of eotaxin/CCL11 from fibroblasts *in vitro*.

Conclusion: Eosinophils mediated the development of murine ICD, possibly through ROS production. Recruitment of eosinophils into the skin was induced by basophils in cooperation with fibroblasts. Our findings introduce the novel concept that basophils promote the recruitment of eosinophils into the skin through fibroblasts in the development of skin inflammation. (J Allergy Clin Immunol 2014;134:100-7.)

Key words: Eosinophil, basophil, fibroblast, eotaxin/CCL11, RANTES/CCL5, irritant contact dermatitis, reactive oxygen species, tumor necrosis factor

Contact dermatitis is one of the most common inflammatory skin diseases and comprises both irritant contact dermatitis (ICD) and allergic contact dermatitis.[1] ICD is more common than allergic contact dermatitis and is responsible for approximately 80% of all cases of contact dermatitis.[2] It is defined as a locally arising reaction that appears after chemical irritant exposure.[2] The chemical agents are directly responsible for cutaneous inflammation because of their inherent toxic properties, which cause tissue injury.[3,4] This inflammatory response is known to activate innate immune system cells, but the precise mechanism of ICD remains largely unknown.

Eosinophils are one of the bone marrow (BM)–derived innate immune leukocytes that normally represent less than 5% of leukocytes in the blood but are frequently detected in the connective tissues and BM.[5] Eosinophils regulate local immune and inflammatory responses, and their accumulation in the blood and tissue is associated with several inflammatory and infectious diseases.[6-8] The recruitment of activated eosinophils from the bloodstream into tissues occurs under numerous conditions and leads to the release of preformed and synthesized products, such as cytokines, chemokines, lipid mediators, cytotoxic granule proteins, and reactive oxygen species (ROS).[7,9] ROS are mainly produced by reduced nicotinamide adenine dinucleotide phosphate oxidase and lead to tissue injury at the inflamed site during allergic inflammation.[10] The differentiation, migration, and activation of eosinophils are mainly enhanced by IL-5.[11] It has been reported that the IL-5–targeted therapy can reduce airway and blood eosinophil counts and prevent asthma exacerbations[12]; however, the roles of eosinophils in the development of cutaneous immune responses remain largely unknown. It has been recently reported that basophils have been detected in patients with skin diseases, including contact dermatitis, in which eosinophils were present.[13,14]

Basophils are one of the least abundant granulocytes, representing less than 1% of peripheral blood leukocytes.[15] Their specific physiologic functions during immune responses have been ignored until recently. Basophils play key roles in the development of acute and chronic allergic responses, protective immunity against parasites, and regulation of acquired immunity, including the augmentation of humoral memory responses.[16,17]

In this study we observed the infiltration of eosinophils in human and murine ICD. Murine ICD responses were attenuated in eosinophil-deficient mice or in mice treated with an ROS inhibitor. ROS was produced by eosinophils, which were attracted by chemokines produced through interaction between basophils

From [a]the Department of Dermatology, Kyoto University Graduate School of Medicine; [b]the Department of Health Chemistry, Graduate School of Pharmaceutical Sciences, University of Tokyo; [c]the Laboratory for Cytokine Regulation, Integrative Medical Science (IMS), RIKEN Yokohama Institute, Kanagawa; and [d]the Division of Molecular Pathology, Research Institute for Biomedical Science, Tokyo University of Science, Chiba.

Supported in part by Grants-in-Aid for Scientific Research from the Ministry of Education, Culture, Sports, Science and Technology and the Ministry of Health, Labor and Welfare of Japan.

Disclosure of potential conflict of interest: The authors declare that they have no relevant conflicts of interest.

Received for publication August 14, 2013; revised February 10, 2014; accepted for publication February 12, 2014.

Available online April 6, 2014.

Corresponding authors: Atsushi Otsuka, MD, PhD and Kenji Kabashima, MD, PhD, Department of Dermatology, Kyoto University Graduate School of Medicine, 54 Shogoin Kawara, Sakyo-ku, Kyoto 606-8507, Japan. E-mail: otsukamn@kuhp.kyoto-u.ac.jp. Or: kaba@kuhp.kyoto-u.ac.jp.

0091-6749/$36.00

http://dx.doi.org/10.1016/j.jaci.2014.02.026

Abbreviations used
APC: Allophycocyanin
Bas TRECK: Basophil-specific enhancer-mediated, toxin receptor-mediated conditional cell knockout
BM: Bone marrow
BMBa: Bone marrow–derived basophil
BMEo: Bone marrow–derived eosinophil
CBA: Cytometric bead array
CM-H_2DCFDA: 5-(and-6)-chloromethyl-2′, 7′-dichlorodihydrofluorescein diacetate
cRPMI: Complete RPMI medium
DT: Diphtheria toxin
Flt3-L: Fms-related tyrosine kinase 3 ligand
H&E: Hematoxylin and eosin
ICD: Irritant contact dermatitis
IgE-CAI: IgE-mediated chronic allergic inflammation
MEF: Mouse embryonic fibroblast
NAC: N-acetylcysteine
PE: Phycoerythrin
RA: Rheumatoid arthritis
ROS: Reactive oxygen species
SCF: Stem cell factor
Tg: Transgenic
TSLP: Thymic stromal lymphopoietin
WT: Wild-type

and fibroblasts. Our findings might raise an important concept that the interaction between basophils and mesenchymal fibroblasts induces the development of ICD through recruitment of eosinophils.

METHODS

Mice

ΔdblGATA mice on a BALB/c background were purchased from the Jackson Laboratory (West Grove, Pa). IL-5 transgenic (Tg) mice on a BALB/c background[18] were kindly provided by Dr K. Takatsu (University of Toyama, Toyama, Japan). Basophil-specific enhancer-mediated, toxin receptor-mediated conditional cell knockout (Bas TRECK) mice on a BALB/c background were generated, as reported previously. Briefly, basophils use a specific 4-kb enhancer fragment containing the 3′ untranslated region and DNase I-hypersensitive site 4 elements to regulate *Il4* gene expression.[19] Using this system, we generated mice that express human diphtheria toxin (DT) receptor under the control of HS4.[17,20] By using these mice, basophils have been reported to play an essential role for the induction and promotion of T_H2 immunity.[17,21] C57BL/6N and BALB/c wild-type (WT) mice were purchased from Japan SLC (Shizuoka, Japan). Eight- to 10-week-old female mice were used for all the experiments and bred in specific pathogen-free facilities at Kyoto University. All experimental procedures were approved by the Institutional Animal Care and Use Committee of Kyoto University Graduate School of Medicine (Kyoto, Japan).

Reagents, antibodies, and flow cytometry

We purchased croton oil and N-acetylcysteine (NAC) from Sigma-Aldrich (St Louis Mo). 5-(and-6)-chloromethyl-2′,7′-dichlorodihydrofluorescein diacetate (CM-H_2DCFDA) was purchased from Invitrogen (Carlsbad, Calif). Recombinant murine stem cell factor (SCF), fms-related tyrosine kinase 3 ligand (Flt3-L), and IL-3 were purchased from PeproTech (Rocky Hill, NJ). Recombinant mouse IL-5 was purchased from R&D Systems (Minneapolis, Minn). Fluorescein isothiocyanate–, phycoerythrin (PE)–, PE-Cy7–, allophycocyanin (APC)–, APC-Cy7–, and Pacific blue–conjugated anti–Gr-1 (RB6-8C5), anti-CD117 (c-Kit; 2B8), anti-FcεRIα (MAR-1), anti-CD49b (Dx5), anti-CD69 (H1.2F3), anti-CD86 (GL1), anti-CD11b (M1/70), and anti-CD45.1 (A20) mAbs were purchased from eBioscience (San Diego, Calif). APC- and PE-conjugated anti–Siglec-F (E50-2440) mAbs were purchased from BD Biosciences (San Jose, Calif). Fluorescein isothiocyanate–conjugated anti–intercellular adhesion molecule 1 (CD54; 3E2) mAb was purchased from BD Biosciences (Franklin Lakes, NJ). Brilliant Violet-conjugated anti-CD45 (30-F11) and purified anti-CD200R3 (Ba13) mAbs and rat anti–mast cell serine protease 8 (TUG8) were purchased from BioLegend (San Diego, Calif). For fluorescence labeling, purified anti-CD200R3 mAb was labeled with the HiLyte Fluor 647 Labeling Kit (Dojindo, Kumamoto, Japan). Functional-grade purified anti-FcεRIα (MAR-1), anti–TNF-α (MP6-XT22), and anti–IL-4 (11B11) mAbs were purchased from eBioscience.

Single-cell suspensions from skin were prepared for flow cytometric analysis as follows. Skin/ear samples were collected by using 8-mm skin biopsy specimens that were cut into pieces and then digested for 1 hour at 37°C in 1.6 mg/mL collagenase type II (Worthington Biochemical, Freehold, NJ) and 0.1 mg/mL DNase I (Sigma-Aldrich) in complete RPMI medium (cRPMI; RPMI 1640 medium [Sigma-Aldrich] containing 10% heat-inactivated FCS [Invitrogen], 0.05 mmol/L 2-mercaptoethanol, 2 mmol/L L-glutamine, 25 mmol/L N-2-hydroxyethylpiperazine-N′-2-ethanesulfonic acid, 1 mmol/L nonessential amino acids, 1 mmol/L sodium pyruvate, 100 U/mL penicillin, and 100 μg/mL streptomycin). Samples were passed through a 40-μm pore size nylon mesh, and cells were stained for the indicated markers. Samples were acquired on a FACSFortessa system (BD Biosciences) and analyzed with FlowJo software (TreeStar, San Carlos, Calif). The numbers of each cell subset were calculated by means of flow cytometry and presented as numbers per square millimeter of skin surface.

ICD and basophil-depletion models

Mice were anesthetized with diethyl ether, and 20 μL of 1% (vol/vol) croton oil in acetone was applied to ear skin. Mice were injected twice daily for 3 days with anti-FcεRIα (MAR-1) to deplete basophils *in vivo*.[22] The efficiency of basophil depletion was analyzed in peripheral blood on day 4. Mice were intraperitoneally injected with NAC (500 mg/kg body weight) and given 20 μL of 50 mmol/L NAC in 100% ethanol on ear skin 1 hour before application of croton oil to block ROS production.

Bas TRECK Tg mice were treated with DT for basophil depletion. BALB/c mice with DT were used as control animals.[20] For DT treatment, mice were injected intraperitoneally with 100 ng of DT per mouse.

Histology and immunohistochemistry

Skin samples for hematoxylin and eosin (H&E) staining were collected from patients with ICD (n = 10) and healthy control subjects (n = 6). The number of eosinophils was counted in 5 fields (20× objective). H&E staining and histologic scoring were evaluated, as previously reported.[23] In brief, samples were scored for the severity and character of the inflammatory response on a subjective grading scale. Responses were graded as follows: 0, no response; 1, minimal response; 2, mild response; 3, moderate response; and 4, marked response. The slides were blinded, randomized, and reread to determine the histologic score. All studies were read by the same pathologist by using the same subjective grading scale. The total histologic score was calculated as the sum of scores, including inflammation, neutrophils, mononuclear cells, edema, and epithelial hyperplasia. The evaluation of eosinophils was performed with Papanicolaou staining.

For the identification of basophils by means of immunohistochemistry, tissue sections were immunostained, as previously reported.[24]

Staining of ROS in ear skin

Mice were treated with 1% croton oil, and cells from the ear skin were isolated 6 hours later and incubated for 30 minutes at 37°C with a solution of 1 μmol/L CM-H_2DCFDA in PBS. After being washed twice with PBS, cells were labeled with anti–Siglec-F and anti-CD11b. We detected production of ROS, as indicated by an increase in 2′,7′-dichlorofluorescein fluorescence.

Preparation of bone marrow–derived basophils, bone marrow–derived eosinophils, and mouse embryonic fibroblasts

cRPMI was used as culture medium. For bone marrow–derived basophil (BMBa) induction, 5×10^6 BM cells were cultured in cRPMI supplemented with 20% FCS in the presence of 10 ng/mL recombinant mouse IL-3 (PeproTech) for approximately 9 to 14 days. For bone marrow–derived eosinophil (BMEo) induction, 1×10^6 BM cells of Ly5.1 mice were cultured in cRPMI supplemented with 20% FCS in the presence of 100 ng/mL recombinant mouse SCF and 100 ng/mL recombinant mouse Flt3-L (PeproTech) from days 0 to 4. On day 4, the medium containing SCF and Flt3-L was replaced with medium containing 10 ng/mL recombinant mouse IL-5 (R&D Systems) thereafter.[25]

Mouse embryonic fibroblasts (MEFs) were obtained from embryos on embryonic day 15 by using standard methods in complete Dulbecco modified Eagle medium (Sigma-Aldrich).[26]

Chemotaxis assay and cell culture

Cells were tested for transmigration to the lower chamber across uncoated 5-μm transwell filters (Corning Costar, Corning, NY) for 3 hours and were enumerated by means of flow cytometry.

BM cells of IL-5 Tg mice and starved BMBas were cocultured at a density of 2×10^5 cells in 200 μL per well in a 96-well microplate at a BM/BMBa ratio of 1:4 in cRPMI supplemented with 10 ng/mL recombinant mouse IL-3 for 24 hours. Separation of BM cells and BMBas was performed by using transwell culture plates with a 3-μm pore size.

MEFs were cultured in 24-well plates to 80% confluence. For coculture, the medium of MEFs was replaced with cRPMI, and the coculture was performed after supplementation with 10 ng/mL recombinant mouse IL-3 for 24 hours.

For inhibition assays, BMBas and MEFs were cocultured with or without 5 μg/mL isotype control antibody (Rat IgG2b, eBioscience), 10 μg/mL anti–IL-4 mAb (11B11, eBioscience), or 5 μg/mL anti–TNF-α mAb (MP6-XT22, eBioscience) for 24 hours.

For chemotaxis toward the supernatant of coculture of BMBas and MEFs, 1×10^6 BM cells were transferred into the upper chamber of a transwell containing 5-μm pore filters. The supernatant of cultivation of MEFs with or without BMBas was added to the lower chamber and incubated for 3 hours at 37°C. Gr-1^{int+}Siglec-$F^+$$CD11b^+$ eosinophils, which migrated to the lower chambers, were counted by using flow cytometry.

ELISA and cytometric bead array

The amount of eotaxin/CCL11 in the culture medium was measured by using ELISA (eBioscience). The amount of RANTES/CCL5 was measured by using a cytometric bead array (CBA) system, according to the manufacturers instructions (BD Biosciences). For measurement of eotaxin and RANTES, a total of 3×10^5 BMBas and 1×10^5 MEFs were cultured with recombinant mouse IL-3 (10 ng/mL) for 24 hours, and the supernatants were collected for ELISA and CBA.

Statistical analysis

Unless otherwise indicated, data are presented as means ± SEMs and a representative of at least 3 independent experiments. *P* values were calculated with the Wilcoxon signed-rank test. *P* values of less than .05 are considered significantly different. A complete description of the methods is available in the Methods section in this article's Online Repository at www.jacionline.org.

RESULTS

Eosinophils play some roles in the development of ICD

We first evaluated whether eosinophils were detected in the lesional skin of patients with ICD. In comparison with healthy donors, the number of eosinophils was significantly higher in

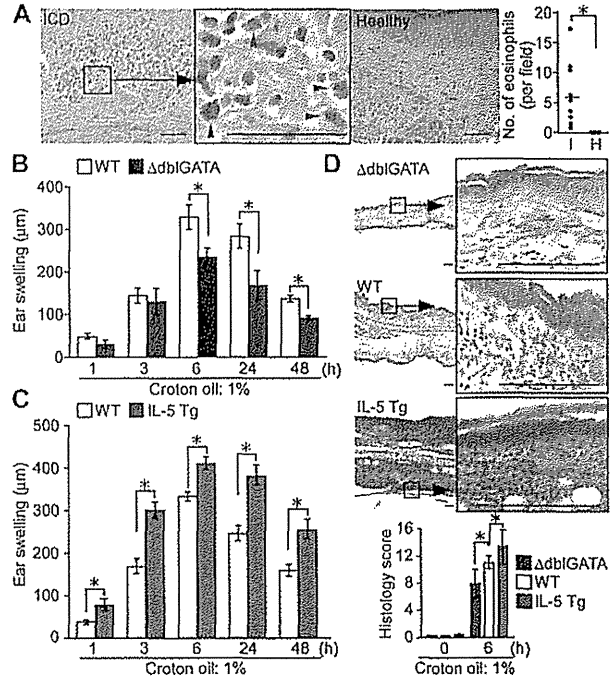

FIG 1. Eosinophils play some role in the development of ICD. A, Histology of the skin of patients with ICD (*I*; n = 10) and healthy donors (*H*; n = 6). The number of eosinophils per field is shown in the *left panel*. *Scale bars* = 50 μm. B and C, Ear swelling of WT and ΔdblGATA mice (n = 9 per group; Fig 1, *B*) and WT (n = 10) and IL-5 Tg (n = 7) mice (Fig 1, *C*) after application of croton oil. D, H&E staining of ears 6 hours after application. Histologic scores of the skin before and 6 hour after application are shown. *Scale bars* = 100 μm. *$P < .05$.

patients with ICD (Fig 1, *A*). To further investigate the role of eosinophils in ICD, we used eosinophil-deficient ΔdblGATA mice.[27] In a croton oil–induced ICD model, the ear-swelling response in ΔdblGATA mice was significantly attenuated compared with that seen in WT mice 6, 24, and 48 hours after application (Fig 1, *B*). To confirm the role of eosinophils in ICD, we used IL-5 Tg mice, which demonstrate eosinophilia in peripheral blood, as well as infiltration of eosinophils into various tissues. The ICD response in IL-5 Tg mice was significantly enhanced compared with that seen in WT mice at 1, 3, 6, 24, and 48 hours after application (Fig 1, *C*). Consistent with the ear-swelling responses, lymphocyte infiltration, including eosinophils, and edema in the dermis 6 hours after application were lower in ΔdblGATA mice and higher in IL-5 Tg mice than in WT mice (Fig 1, *D*, and see Tables E1 and E2 in this article's Online Repository at www.jacionline.org). In addition, major eosinophil chemoattractants, such as RANTES and eotaxin, were detected in the skin after croton oil application (see Fig E1 in this article's Online Repository at www.jacionline.org).

Eosinophils produce ROS in patients with ICD

ROS is known to induce the development of some inflammatory conditions.[28] To assess the role of ROS in the ICD model, we used the ROS inhibitor NAC. Ear swelling significantly decreased after NAC treatment in both WT and ΔdblGATA mice (Fig 2, *A*). Of note, ear swelling in NAC-treated WT mice was comparable with that seen in NAC-treated ΔdblGATA mice, suggesting that

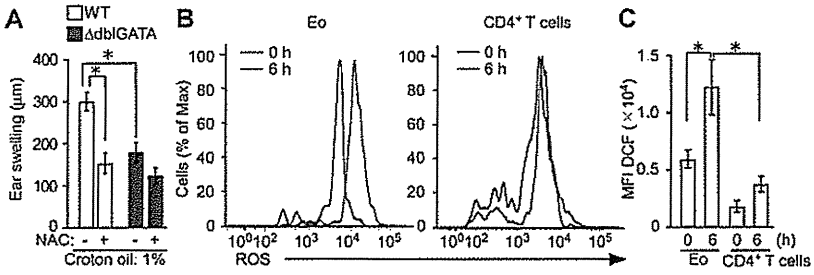

FIG 2. ICD is mediated by eosinophil-derived ROS. A, Ear swelling of WT (n = 11) and ΔdblGATA (n = 7) mice pretreated with or without antioxidant NAC measured 24 hours after application. B and C, Histogram (Fig 2, *B*) and mean fluorescence intensity *(MFI)* of 2',7'-dichlorofluorescein *(DCF;* Fig 2, *C*) on Siglec-F$^+$CD11b$^+$ eosinophils and CD4$^+$ T cells before (ie, steady states; 0 hours) or 6 hours after application. *$P < .05$.

ROS produced from eosinophils play a major role in the induction of ICD. In addition, using the ROS-sensitive fluorescent dye CM-H_2DCFDA, we detected a significant amount of ROS production by eosinophils in the skin under steady-state conditions. In addition, eosinophils in the ICD lesional skin expressed higher amounts of ROS, which were also higher than those seen in infiltrated CD4$^+$ T cells (Fig 2, *B* and *C*).[20]

Basophils enhance eosinophil recruitment into the skin

Basophils tended to be detected in patients with skin diseases when eosinophils were present.[13] We next analyzed the distribution of eosinophils and basophils by using Papanicolaou staining and immunohistochemistry, respectively, in the ICD model. Mcp8$^+$ basophils were localized in the vicinity of eosinophils in the inflamed skin (Fig 3, *A*). We further evaluated whether basophils were detected in the lesional skin of patients with ICD and demonstrated the coincidental presence of basophils and eosinophils in inflamed skin of human patients with ICD (see Fig E2 in this article's Online Repository at www.jacionline.org). In addition, the numbers of neutrophils and basophils in ΔdblGATA mice were comparable with those in WT mice 6 hours after croton oil application (Fig 3, *B* and *C*), which suggests that eosinophils do not affect the recruitment of neutrophils and basophils into the skin.

We further analyzed the kinetics of recruitment of eosinophils and basophils in the lesional skin with ICD. Basophil numbers increased 3 hours after croton oil application. On the other hand, eosinophil numbers increased 24 hours after croton oil application, the timing of which was later than that of basophils (Fig 3, *D*).

Therefore we hypothesized that basophils affect eosinophil infiltration during ICD. To address this hypothesis, we depleted basophils with anti-FcεRIα (MAR-1) antibody.[22] Administration of anti-FcεRIα antibodies significantly suppressed ear swelling and infiltration of eosinophils, but not neutrophils or mast cells, into the skin (Fig 3, *E* and *F*, and see Fig E3 in this article's Online Repository at www.jacionline.org). To confirm these results, we next used Bas TRECK Tg mice to deplete basophils conditionally.[17,20] Consistently, ear-swelling responses and numbers of infiltrating eosinophils, but not neutrophils, in DT-treated Bas TRECK Tg mice were significantly attenuated compared with those in DT-treated WT mice (Fig 3, *G* and *H*, and see Fig E4 in this article's Online Repository at www.jacionline.org). Similar findings were observed in mast cell–deficient WBB6F$_1$-*Kit*$^{W/Wv}$ (W/Wv) mice (see Fig E5 in this article's Online Repository at www.jacionline.org). These findings suggest the potential overlap of mast cells and basophils.

Basophils augment eosinophil activation

Impaired eosinophil recruitment as a result of depletion of basophils suggests that basophils promote eosinophil infiltration into the skin. To address this issue, we prepared BM cells from IL-5 Tg mice that included numerous eosinophils and incubated them with or without BMBas for 24 hours. Cocultivation of BM cells with BMBas significantly enhanced expression levels of activation markers, CD69, CD86, and intercellular adhesion molecule 1, on eosinophils among BM cells (Fig 4).[30-32] On the other hand, the incubation of BMBas and BM cells of IL-5 Tg mice separately using transwells did not induce upregulation of the above activation markers on eosinophils (Fig 4). These findings suggest that basophils require direct cell-to-cell interaction to activate eosinophils.

Basophils promote recruitment of eosinophils in cooperation with fibroblasts

Next, we evaluated whether basophils were capable of attracting eosinophils. We prepared BMBas and BMEos for chemotaxis assay. The chemotaxis of BMEos applied to the upper chamber was significantly enhanced when BMBas were added to the lower chamber (Fig 5, *A*). On the other hand, BMBas applied to the upper chamber did not migrate to the lower chamber, where BMEos were added (Fig 5, *A*). These results suggest that basophils attract eosinophils but not *vice versa*.

We then sought to identify how basophils recruit eosinophils. CCR3 is known to mediate eosinophil chemotaxis in response to eotaxin and RANTES.[33] The number of eosinophils in anti-CCR3 antibody–treated mice was attenuated compared with that seen in control antibody-treated mice 24 hours after croton oil application (see Fig E6, *A*, in this article's Online Repository at www.jacionline.org). In addition, amounts of RANTES and eotaxin in the skin after croton oil application were reduced in basophil-depleted mice using a Bas TRECK Tg system (see Fig E6, *B*). RANTES was detected in the supernatant medium of IL-3–stimulated BMBa cultures (Fig 5, *B*), but eotaxin was not detected therein (data not shown).

Fibroblasts are known to produce chemoattractants, such as RANTES and eotaxin.[34] We observed that BMBas expressed only RANTES mRNA, which was consistent with the findings in

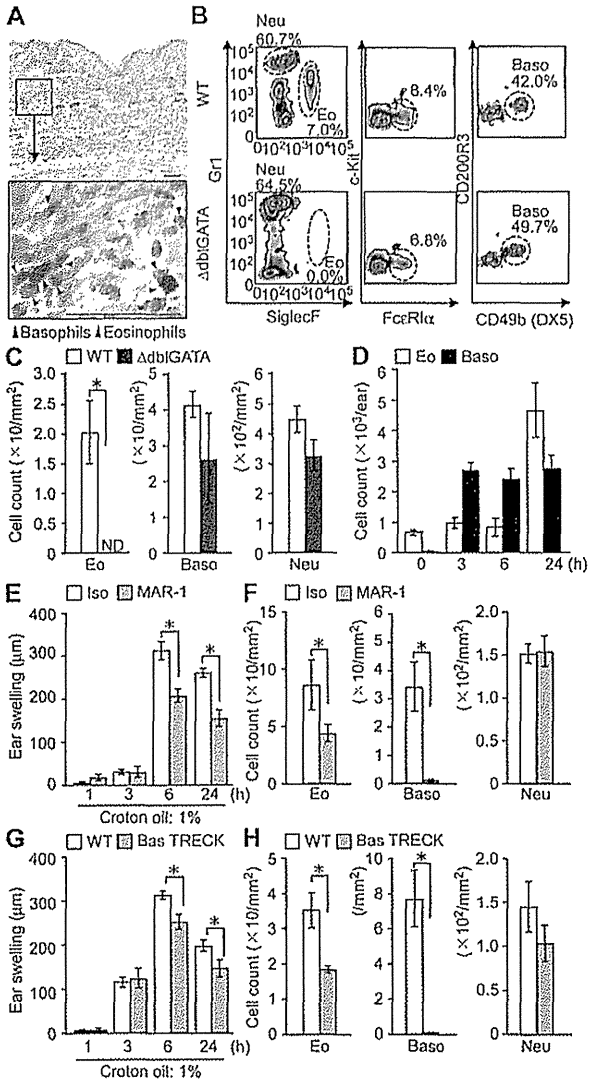

FIG 3. Basophils accumulate in the skin before eosinophil infiltration in ICD. A, Mcp8^{+} basophils *(black arrowheads)* and Papanicolaou staining–positive eosinophils *(red arrowheads)* 24 hours after croton oil application. *Scale bars* = 50 μm. B and C, Fluorescence-activated cell sorting plots (Fig 3, *B*) and numbers (Fig 3, *C*) of infiltrating eosinophils *(Eo)*, basophils *(Baso)*, and neutrophils *(Neu)* of WT and ΔdblGATA mice per square millimeter of surface of the skin 6 hours after croton oil application. D, Kinetics of the numbers of eosinophils and basophils in the skin. E and F, Ear swelling (Fig 3, *E*) and cell infiltration (Fig 3, *F*) in ICD determined by means of depletion of basophils by MAR-1 antibody (n = 5 per group). G and H, Ear swelling in ICD (Fig 3, *G*) and cell infiltration (Fig 3, *H*) of WT (n = 5) and Bas TRECK Tg (n = 4) mice 24 hours after croton oil application. *P < .05.

Fig 5, *B*, and that MEFs expressed RANTES and eotaxin mRNA using quantitative PCR (see Fig E7 in this article's Online Repository at www.jacionline.org). Because basophils infiltrated into the dermis in which mesenchymal fibroblasts localize abundantly, we then evaluated the effect of the interaction between basophils and fibroblasts on chemokine production. Although MEFs expressed marginal RANTES in the culture supernatant, BMBas expressed pronounced RANTES. Cocultivation of MEFs significantly increased RANTES levels in the culture supernatant of BMBas (Fig 5, *C*).

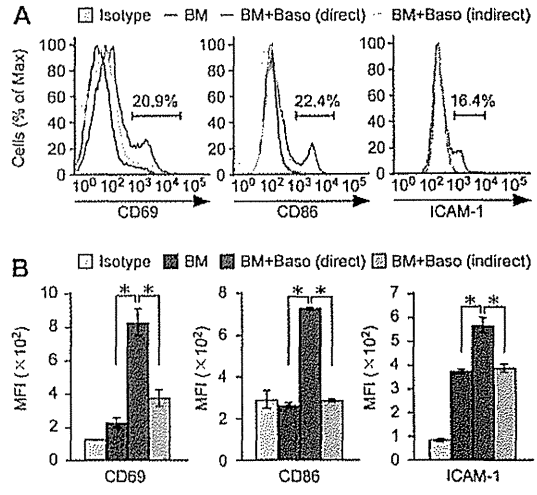

FIG 4. Basophils promote the activation of eosinophils through direct cell interaction. Histogram (A) and mean fluorescence intensity *(MFI;* B) of CD69, CD86, and intercellular adhesion molecule 1 *(ICAM-1)* expression on the eosinophil subset in BM cells of IL-5 Tg mice cultured with or without BMBas directly or indirectly. *P < .05.

It has been reported that TNF-α promotes migration of immune cells, such as dendritic cells and mast cells,[35] and that IL-4 is an inducer for several chemokines.[36] We next hypothesized that TNF-α or IL-4 might mediate the production of RANTES by basophils. To address this issue, we examined whether enhanced RANTES production in cocultivation of BMBas and MEFs was inhibited by anti–TNF-α or anti–IL-4 antibody. Although anti–IL-4 antibody did not inhibit RANTES production, anti–TNF-α antibody inhibited RANTES production in the culture supernatant of basophils and cocultivation of basophils and MEFs (Fig 5, *C*).

Next, we sought to reveal the mechanism by which eotaxin is induced in the skin. In contrast to RANTES, eotaxin mRNA was strongly detected in MEFs (see Fig E7), whereas eotaxin protein levels in the culture supernatant of MEFs were marginal (Fig 5, *D*). Interestingly, eotaxin protein was induced by cocultivation of BMBas and MEFs (Fig 5, *D*). Differently from RANTES induction, both anti–IL-4 antibody and anti–TNF-α antibody inhibited the induction of eotaxin. We found that the main producer of TNF-α and IL-4 was IL-3–stimulated BMBas (Fig 5, *E*). Consistently, the amounts of IL-4 and TNF-α in the skin were reduced by depletion of basophils after croton oil application (see Fig E8 in this article's Online Repository at www.jacionline.org). In addition, cocultivation of BMBas and MEFs in the presence of IL-3 to the lower chamber attracted eosinophils applied to the upper chamber when compared with only BMBa or only MEF incubation to the lower chamber (Fig 5, *F*).

DISCUSSION

In this study we demonstrated that eosinophils mediate the development of ICD reactions, possibly through ROS production. Eosinophils accumulate into human and murine ICD skin lesions in the vicinity of basophils. Basophils are detected in the skin lesion before eosinophil infiltration, suggesting that basophils promote eosinophil accumulation into the skin. Consistently, BMBas promote the migration and activation of eosinophils *in vitro*. RANTES is produced by IL-3–stimulated basophils and

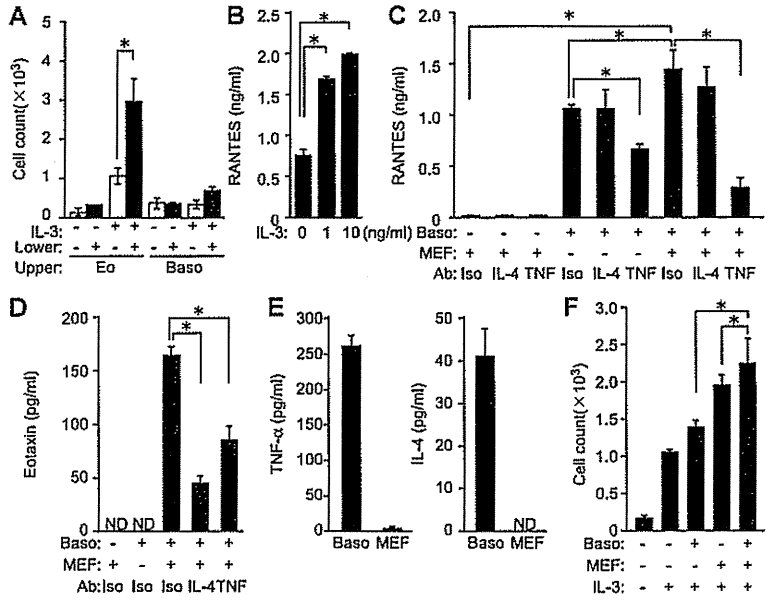

FIG 5. Basophils promote eosinophil recruitment directly or indirectly through fibroblasts. **A**, Migration of eosinophils and basophils. BMBas or BMEos were applied to the upper or lower chambers with or without IL-3, and cell numbers were evaluated. **B**, Amount of RANTES in the supernatants of BMBa cultures with or without IL-3. **C** and **D**, Amount of RANTES (Fig 5, *C*) and eotaxin (Fig 5, *D*) in supernatants of MEFs, BMBas *(Baso)*, or MEFs plus BMBas for 24 hours with or without neutralizing anti–IL-4 or anti–TNF-α antibodies. **E**, Amount of TNF-α and IL-4 in supernatants of BMBa or MEF cultures. **F**, Number of migrating eosinophils. Chemotaxis of eosinophils in the lower chamber that were incubated with MEFs, BMBas, or MEF plus BMBas in the presence or absence of IL-3 was evaluated. *ND*, Not determined. $*P < .05$.

even more by cocultivation of MEFs in a TNF-α–dependent manner. On the other hand, eotaxin is produced by cocultivation of BMBas and MEFs, which is inhibited by anti–TNF-α and anti–IL-4 antibody. Basophils attracted eosinophils through CCR3, and direct cell-to-cell interaction was required for activation of eosinophils by basophils. Taken together, our findings suggest that basophils infiltrating into the skin attract eosinophils directly or indirectly through interaction of mesenchymal fibroblasts and that basophils activate eosinophils *in situ*, which contributes to the development of skin inflammation (see Fig E9 in this article's Online Repository at www.jacionline.org).

Basophils are thought to be major early producers of IL-4 and IL-13, which are critical for triggering and maintaining allergic responses.[17,37] In this report we have demonstrated that basophils rapidly infiltrate into the inflamed skin and subsequently attract eosinophils therein for the development of ICD.

IgE-mediated chronic allergic inflammation (IgE-CAI) is a long-lasting inflammation that follows immediate-type reactions and late-phase responses. It is histopathologically characterized by massive eosinophil infiltration into the skin.[38] Basophils are considered to be cells responsible for initiating inflammation of IgE-CAI. Consistent with our results using ICD, the number of eosinophils increased in the lesional skin after basophil infiltration in IgE-CAI.[39] In addition, basophils colocalize with eosinophils in human skin diseases, such as atopic dermatitis and eosinophilic pustular folliculitis.[40] These findings suggest that our novel findings might be applicable to more general skin inflammatory diseases both in mice and human subjects.

In this study we have clarified that basophils recruit eosinophils into the skin. The next question is how basophils infiltrate into the lesional skin. It has been reported that α(1,3) fucosyltransferases IV and VII are essential for the initial recruitment of basophils in patients with chronic allergic inflammation.[41] We are currently working to understand the underlying mechanism of how basophils infiltrate into the lesion as an inducer of skin inflammation in our model.

Both basophils and eosinophils express the common chemokine receptor CCR3. Ligands for CCR3, such as eotaxin, are produced by dermal fibroblasts in response to T_H2-type cytokines in human subjects.[42] We demonstrated herein a new network for eosinophil infiltration into the skin, as summarized in Fig E9. Activated basophils produced RANTES, which was dependent on TNF-α that was possibly produced by basophils themselves. In addition, basophils that have infiltrated into the lesional skin were activated through contact with dermal fibroblasts and produced IL-4 and TNF-α, which promoted eotaxin expression from fibroblasts. These cytokine-chemokine networks might support recruitment of eosinophils from the bloodstream into the skin.

It has been reported that ICD is IgE independent.[43] In addition, recent studies showed that thymic stromal lymphopoietin (TSLP), which is produced by keratinocytes and fibroblasts in the skin, activated basophils.[17,44] We have demonstrated that croton oil application promoted the induction of TSLP in ICD (data not shown). Therefore we assume that TSLP is one of the candidates for the activator in this assay.

In this study we also examined the role of mast cells in ICD by using mast cell–deficient $Kit^{W/Wv}$ mice. Interestingly, similar phenotypes, such as the attenuation of ICD and eosinophil infiltration, were found in a mast cell–deficient model (see Fig E5). These findings suggest the potential overlap of mast cells and basophils, which seems to be intriguing. We demonstrated

that TNF-α was decreased partially, but IL-4 was almost completely diminished by basophil depletion (see Fig E8). These findings suggest that TNF-α and IL-4 might be released by mast cells and basophils, respectively, for the development of ICD.

TNF-α is a potent proinflammatory and immunomodulatory cytokine implicated in inflammatory conditions. Treatment with anti–TNF-α antibody is effective for several diseases, including psoriasis, Crohn disease, and rheumatoid arthritis (RA). On the other hand, peripheral blood eosinophilia can be observed in patients with active inflammatory RA.[45] We demonstrated herein that anti–TNF-α antibody inhibited the production of eosinophil chemoattractants, such as RANTES and eotaxin, from basophils and fibroblasts (Fig 5, *C* and *D*). Because synovial fibroblasts and basophils have been reported to play important roles in the pathogenesis of RA,[46] anti–TNF-α might also block the interaction of basophils, eosinophils, and fibroblasts to regulate RA activity. Further understanding of the relationship between basophils, eosinophils, and fibroblasts in the immune organs might lead to the development of new therapeutic strategies to control eosinophil-associated diseases, such as ICD, atopic dermatitis, and allergic asthma.

We thank Dr Hideaki Tanizaki, Dr Kazunari Sugita, Ms Kaori Tomari, Ms Kiiko Kumagai, Ms Natsuki Ishizawa, and Ms Hiromi Doi for technical assistance.

Clinical implications: Basophils initiate the recruitment of eosinophils into the skin through fibroblasts. Interference of this system might control several skin inflammations.

REFERENCES

1. Honda T, Egawa G, Grabbe S, Kabashima K. Update of immune events in the murine contact hypersensitivity model: toward the understanding of allergic contact dermatitis. J Invest Dermatol 2013;133:303-15.
2. Nosbaum A, Vocanson M, Rozieres A, Hennino A, Nicolas JF. Allergic and irritant contact dermatitis. Eur J Dermatol 2009;19:325-32.
3. Egawa G, Honda T, Tanizaki H, Doi H, Miyachi Y, Kabashima K. In vivo imaging of T-cell motility in the elicitation phase of contact hypersensitivity using two-photon microscopy. J Invest Dermatol 2011;131:977-9.
4. Egawa G, Kabashima K. Skin as a peripheral lymphoid organ: revisiting the concept of skin-associated lymphoid tissues. J Invest Dermatol 2011;131:2178-85.
5. Kita H. Eosinophils: multifaceted biological properties and roles in health and disease. Immunol Rev 2011;242:161-77.
6. Rosenberg HF, Dyer KD, Foster PS. Eosinophils: changing perspectives in health and disease. Nat Rev Immunol 2013;13:9-22.
7. Cheung PF, Wong CK, Ho AW, Hu S, Chen DP, Lam CW. Activation of human eosinophils and epidermal keratinocytes by Th2 cytokine IL-31: implication for the immunopathogenesis of atopic dermatitis. Int Immunol 2010;22:453-67.
8. Nakahigashi K, Doi H, Otsuka A, Hirabayashi T, Murakami M, Urade Y, et al. PGD$_2$ induces eotaxin-3 via PPARγ from sebocytes: a possible pathogenesis of eosinophilic pustular folliculitis. J Allergy Clin Immunol 2012;129:536-43.
9. Mori M, Takaku Y, Kobayashi T, Hagiwara K, Kanazawa M, Nagata M. Eosinophil superoxide anion generation induced by adhesion molecules and leukotriene D4. Int Arch Allergy Immunol 2009;149(suppl 1):31-8.
10. Nathan C, Cunningham-Bussel A. Beyond oxidative stress: an immunologist's guide to reactive oxygen species. Nat Rev Immunol 2013;13:349-61.
11. Yamaguchi Y, Hayashi Y, Sugama Y, Miura Y, Kasahara T, Kitamura S, et al. Highly purified murine interleukin 5 (IL-5) stimulates eosinophil function and prolongs in vitro survival. IL-5 as an eosinophil chemotactic factor. J Exp Med 1988;167:1737-42.
12. Liu Y, Zhang S, Li D-W, Jiang S-J. Efficacy of anti-interleukin-5 therapy with mepolizumab in patients with asthma: a meta-analysis of randomized placebo-controlled trials. PloS One 2013;8:e59872.
13. Ito Y, Satoh T, Takayama K, Miyagishi C, Walls A, Yokozeki H. Basophil recruitment and activation in inflammatory skin diseases. Allergy 2011;66:1107-13.
14. Dvorak HF, Mihm MC. Basophilic leukocytes in allergic contact dermatitis. J Exp Med 1972;135:235-54.
15. Schroeder JT. Basophils: emerging roles in the pathogenesis of allergic disease. Immunol Rev 2011;242:144-60.
16. Denzel A, Maus UA, Rodriguez Gomez M, Moll C, Niedermeier M, Winter C, et al. Basophils enhance immunological memory responses. Nat Immunol 2008; 9:733-42.
17. Otsuka A, Nakajima S, Kubo M, Egawa G, Honda T, Kitoh A, et al. Basophils are required for the induction of Th2 immunity to haptens and peptide antigens. Nat Commun 2013;4:1738.
18. Tominaga A, Takaki S, Koyama N, Katoh S, Matsumoto R, Migita M, et al. Transgenic mice expressing a B cell growth and differentiation factor gene (interleukin 5) develop eosinophilia and autoantibody production. J Exp Med 1991;173:429-37.
19. Yagi R, Tanaka S, Motomura Y, Kubo M. Regulation of the Il4 gene is independently controlled by proximal and distal 3' enhancers in mast cells and basophils. Mol Cell Biol 2007;27:8087-97.
20. Sawaguchi M, Tanaka S, Nakatani Y, Harada Y, Mukai K, Matsunaga Y, et al. Role of mast cells and basophils in IgE responses and in allergic airway hyperresponsiveness. J Immunol 2012;188:1809-18.
21. Noti M, Wojno EDT, Kim BS, Siracusa MC, Giacomin PR, Nair MG, et al. Thymic stromal lymphopoietin-elicited basophil responses promote eosinophilic esophagitis. Nat Med 2013;19:1005-13.
22. Tang H, Cao W, Kasturi SP, Ravindran R, Nakaya HI, Kundu K, et al. The T helper type 2 response to cysteine proteases requires dendritic cell-basophil cooperation via ROS-mediated signaling. Nat Immunol 2010;11:608-17.
23. Nakajima S, Honda T, Sakata D, Egawa G, Tanizaki H, Otsuka A, et al. Prostaglandin I2-IP signaling promotes Th1 differentiation in a mouse model of contact hypersensitivity. J Immunol 2010;184:5595-603.
24. Ugajin T, Kojima T, Mukai K, Obata K, Kawano Y, Minegishi Y, et al. Basophils preferentially express mouse Mast Cell Protease 11 among the mast cell tryptase family in contrast to mast cells. J Leukoc Biol 2009;86:1417-25.
25. Dyer KD, Moser JM, Czapiga M, Siegel SJ, Percopo CM, Rosenberg HF. Functionally competent eosinophils differentiated ex vivo in high purity from normal mouse bone marrow. J Immunol 2008;181:4004-9.
26. Sato T, Saito R, Jinushi T, Tsuji T, Matsuzaki J, Koda T, et al. IFN-gamma-induced SOCS-1 regulates STAT6-dependent eotaxin production triggered by IL-4 and TNF-alpha. Biochem Biophys Res Commun 2004;314:468-75.
27. Yu C, Cantor AB, Yang H, Browne C, Wells RA, Fujiwara Y, et al. Targeted deletion of a high-affinity GATA-binding site in the GATA-1 promoter leads to selective loss of the eosinophil lineage in vivo. J Exp Med 2002;195: 1387-95.
28. Nagata M. Inflammatory cells and oxygen radicals. Curr Drug Targets Inflamm Allergy 2005;4:503-4.
29. Schuessel K, Frey C, Jourdan C, Keil U, Weber CC, Muller-Spahn F, et al. Aging sensitizes toward ROS formation and lipid peroxidation in PS1M146L transgenic mice. Free Radic Biol Med 2006;40:850-62.
30. Ochkur SI, Jacobsen EA, Protheroe CA, Biechele TL, Pero RS, McGarry MP, et al. Coexpression of IL-5 and eotaxin-2 in mice creates an eosinophil-dependent model of respiratory inflammation with characteristics of severe asthma. J Immunol 2007; 178:7879-89.
31. Wang H-B, Ghiran I, Matthaei K, Weller PF. Airway eosinophils: allergic inflammation recruited professional antigen-presenting cells. J Immunol 2007; 179:7585-92.
32. Duez C, Dakhama A, Tomkinson A, Marquillies P, Balhorn A, Tonnel A-B, et al. Migration and accumulation of eosinophils toward regional lymph nodes after airway allergen challenge. J Allergy Clin Immunol 2004;114:820-5.
33. Mould AW, Matthaei KI, Young IG, Foster PS. Relationship between interleukin-5 and eotaxin in regulating blood and tissue eosinophilia in mice. J Clin Invest 1997; 99:1064-71.
34. Mochizuki M, Schroder J, Christophers E, Yamamoto S. IL-4 induces eotaxin in human dermal fibroblasts. Int Arch Allergy Immunol 1999;120(suppl 1):19-23.
35. Otsuka A, Kubo M, Honda T, Egawa G, Nakajima S, Tanizaki H, et al. Requirement of interaction between mast cells and skin dendritic cells to establish contact hypersensitivity. PLoS One 2011;6:e25538.
36. Nelms K, Keegan AD, Zamorano J, Ryan JJ, Paul WE. The IL-4 receptor: signaling mechanisms and biologic functions. Annu Rev Immunol 1999;17:701-38.
37. Perrigoue JG, Saenz SA, Siracusa MC, Allenspach EJ, Taylor BC, Giacomin PR, et al. MHC class II-dependent basophil-CD4+ T cell interactions promote T(H)2 cytokine-dependent immunity. Nat Immunol 2009;10:697-705.
38. Obata K, Mukai K, Tsujimura Y, Ishiwata K, Kawano Y, Minegishi Y, et al. Basophils are essential initiators of a novel type of chronic allergic inflammation. Blood 2007;110:913-20.
39. Mukai K, Matsuoka K, Taya C, Suzuki H, Yokozeki H, Nishioka K, et al. Basophils play a critical role in the development of IgE-mediated chronic allergic inflammation independently of T cells and mast cells. Immunity 2005;23:191-202.

40. Otsuka A, Miyagawa-Hayashino A, Walls AF, Miyachi Y, Kabashima K. Comparison of basophil infiltration into the skin between eosinophilic pustular folliculitis and neutrophilic folliculitis. J Eur Acad Dermatol Venereol 2012;26: 527-9.
41. Saeki K, Satoh T, Yokozeki H. α (1, 3) Fucosyltransferases IV and VII are essential for the initial recruitment of basophils in chronic allergic inflammation. J Invest Dermatol 2013;133:2161-9.
42. Rokudai A, Terui Y, Kuniyoshi R, Mishima Y, Mishima Y, Aizu-Yokota E, et al. Differential regulation of eotaxin-1/CCL11 and eotaxin-3/CCL26 production by the TNF-alpha and IL-4 stimulated human lung fibroblast. Biol Pharm Bull 2006;29:1102-9.
43. Bryce PJ, Miller ML, Miyajima I, Tsai M, Galli SJ, Oettgen HC. Immune sensitization in the skin is enhanced by antigen-independent effects of IgE. Immunity 2004;20:381-92.
44. Siracusa MC, Saenz SA, Hill DA, Kim BS, Headley MB, Doering TA, et al. TSLP promotes interleukin-3-independent basophil haematopoiesis and type 2 inflammation. Nature 2011;477:229-33.
45. Aloush V, George J, Elkayam O, Wigler I, Oren S, Entin-Meer M, et al. Decreased levels of CCR3 in CD4+ lymphocytes of rheumatoid arthritis patients. Clin Exp Rheumatol 2010;28:462-7.
46. Schuerwegh AJ, Ioan-Facsinay A, Dorjee AL, Roos J, Bajema IM, van der Voort EI, et al. Evidence for a functional role of IgE anticitrullinated protein antibodies in rheumatoid arthritis. Proc Natl Acad Sci U S A 2010;107:2586-91.

Allergy EUROPEAN JOURNAL OF ALLERGY AND CLINICAL IMMUNOLOGY EAACI

Allergy

REVIEW

Mast cells and basophils in cutaneous immune responses

A. Otsuka[1] & K. Kabashima[1,2]

[1]Department of Dermatology, Kyoto University Graduate School of Medicine, Kyoto; [2]PRESTO, Japan Science and Technology Agency, Kawaguchi, Saitama, Japan

To cite this article: Otsuka A, Kabashima K. Mast cells and basophils in cutaneous immune responses. *Allergy* 2015; **70**: 131–140.

Keywords
allergic contact dermatitis; atopic dermatitis; basophil; mast cell.

Correspondence
Kenji Kabashima, MD, PhD, Department of Dermatology, Kyoto University Graduate School of Medicine, 54 Shogoin Kawara, Sakyo-ku, Kyoto 606-8507, Japan.
Tel.: +81-75-751-3310
Fax: +81-75-761-3002
E-mail: kaba@kuhp.kyoto-u.ac.jp

Accepted for publication 17 September 2014

DOI:10.1111/all.12526

Edited by: Hans-Uwe Simon

Abstract

Mast cells and basophils share some functions in common and are generally associated with T helper 2 (Th2) immune responses, but taking basophils as surrogate cells for mast cell research or vice versa for several decades is problematic. Thus far, their *in vitro* functions have been well studied, but their *in vivo* functions remained poorly understood. New research tools for their functional analysis *in vivo* have revealed previously unrecognized roles for mast cells and basophils in several skin disorders. Newly developed mast cell-deficient mice provided evidence that mast cells initiate contact hypersensitivity via activating dendritic cells. In addition, studies using basophil-deficient mice have revealed that basophils were responsible for cutaneous Th2 skewing to haptens and peptide antigens but not to protein antigens. Moreover, human basophils infiltrate different skin lesions and have been implicated in the pathogenesis of skin diseases ranging from atopic dermatitis to autoimmune diseases. In this review, we will discuss the recent advances related to mast cells and basophils in human and murine cutaneous immune responses.

Mast cells and basophils are in some respects similar and are generally associated with T helper 2 (Th2) immune responses, which are mainly characterized by the presence of Th2 cells and high levels of immunoglobulin E (IgE). Th2 immunity develops in response to allergens and parasites. Mast cells and basophils express several effector molecules in common, including mast cell-associated proteases, vasodilating substances such as histamine, various cytokines, pro-inflammatory chemokines, and lipid mediators. Many of these effector molecules are rapidly released in response to the activation of the high-affinity receptor for IgE (FcεRI) or other surface receptors that are expressed on mast cells and basophils (1, 2).

Previous studies have reported the involvement of mast cells in other processes such as protection of the host against a range of parasitic and bacterial infections, degradation of toxins, induction of tolerance to skin transplants, and tumor rejection. Conversely, they cause detrimental inflammatory responses to allergens and might also exacerbate autoimmunity (3). Basophils can contribute to protection against helminths and ticks (4), but they can also play a pivotal role during IgE-mediated chronic allergic inflammation of the skin and are implicated in the late-phase response of allergic asthma (5).

In addition to their effector functions, basophils and mast cells can rapidly respond to the environmental signals and might function as modulators of immune responses by enhancing, suppressing, or polarizing the adaptive immunity (2, 3, 6, 7).

Taking basophils as surrogate cells for mast cell research or vice versa is problematic for many reasons. Their development, distribution, and proliferation are different as summarized in Table 1. Mast cells are widely distributed throughout tissues, especially near surfaces exposed to the environment, such as the skin, airways, and gastrointestinal and genitourinary tracts, where pathogens, allergens, and other environmental agents are encountered (8). On the other hand, basophils are primarily found in the blood circulation under steady-state conditions and are mobilized to the blood, spleen, lungs, and liver in response to inflammatory signals that rapidly induce basophil expansion in the bone marrow. In addition, the lifespan of basophils is short, but mast cells can survive for a long time, and some tissue mast cells proliferate *in situ* in response to certain form of stimulation (9).

Although a number of functions of mast cells or basophils have been reported, the physiologic *in vivo* functions of both cell types are still largely unknown due to the fact that these cells are rare and are difficult to isolate as pure populations without interfering with their activation. Furthermore, there have been no ideal tools to evaluate their *in vivo* role, such as